Molecular Biology of the Cell
Vol. 19, 3052–3069, July 2008

Novel Genetic Tools Reveal Cdk5's Major Role in Golgi Fragmentation in Alzheimer's Disease

Kai-Hui Sun,* Yolanda de Pablo,* Fabien Vincent,† Emmanuel O. Johnson, Angela K. Chavers, and Kavita Shah

Department of Chemistry and Purdue Cancer Center, Purdue University, West Lafayette, IN 47907

Submitted November 5, 2007; Revised April 15, 2008; Accepted May 5, 2008
Monitoring Editor: Vivek Malhotra

Golgi fragmentation is a common feature in multiple neurodegenerative diseases; however, the precise mechanism that causes fragmentation remains obscure. A potential link between Cdk5 and Golgi fragmentation in Alzheimer's disease (AD) was investigated in this study. Because Golgi is physiologically fragmented during mitosis by Cdc2 kinase and current Cdk5-specific chemical inhibitors target Cdc2 as well, development of novel tools to modulate Cdk5 activity was essential. These enzyme modulators, created by fusing TAT sequence to Cdk5 activators and an inhibitor peptide, enable specific activation and inhibition of Cdk5 activity with high temporal control. These genetic tools revealed a major role of Cdk5 in Golgi fragmentation upon β-amyloid and glutamate stimulation in differentiated neuronal cells and primary neurons. A crucial role of Cdk5 was further confirmed when Cdk5 activation alone resulted in robust Golgi disassembly. The underlying mechanism was unraveled using a chemical genetic screen, which yielded *cis*-Golgi matrix protein GM130 as a novel substrate of Cdk5. Identification of the Cdk5 phosphorylation site on GM130 suggested a mechanism by which Cdk5 may cause Golgi fragmentation upon deregulation in AD. As Cdk5 is activated in several neurodegenerative diseases where Golgi disassembly also occurs, this may be a common mechanism among multiple disorders.

INTRODUCTION

Golgi fragmentation manifests itself in several neurodegenerative diseases including Alzheimer's disease (AD), Parkinson's disease (PD), amyotropic lateral sclerosis (ALS), corticobasal degeneration, spinocerebelar ataxia type 2 (SCA2), and Creutzfeldt-Jakob disease (Gonatas *et al.*, 2006). In contrast to pathological Golgi fragmentation, physiological Golgi disassembly is a highly orchestrated process that is essential for entry into mitosis (Sutterlin *et al.*, 2002; Colanzi *et al.*, 2003; Altan-Bonnet *et al.*, 2004). A number of kinases such as Cdc2, RAF/MEK1/ERK1c, Plk1, and Plk3 have been shown to phosphorylate several Golgi proteins that promote Golgi dispersion during mitosis (Acharya *et al.*, 1998; Sutterlin *et al.*, 2001; Xie *et al.*, 2004; Shaul and Seger, 2006; Colanzi and Corda, 2007). Although mitotic Golgi fragments reassemble after cytokinesis, Golgi fragmentation during apoptosis is irreversible. Apoptotic Golgi dispersion is due to caspase-mediated proteolytic cleavage of several Golgi proteins such as golgin-160, GM130, GRASP65, p115, syntaxin 5, and giantin (Mancini *et al.*, 2000; Chiu *et al.*, 2002; Lane *et al.*, 2002; Lowe *et al.*, 2004; Walker *et al.*, 2004; Mukherjee *et al.*, 2007). These findings suggest that Golgi fragmentation during neurodegeneration may follow a similar route. However, recent studies suggest that Golgi fragmentation in neurodegeneration, rather than being a consequence of apoptosis, may be an early and irreversible trigger for apoptosis (Gonatas *et al.*, 2006; Nakagomi *et al.*, 2008). Golgi fragmentation in PD occurs before the aggregation of fibrillar mutant α-synuclein, supporting this hypothesis. In AD, Golgi fragmentation and mitochondrial dysfunction coexist in neurons that lack neurofibrillary tangles (NFT), suggesting that these events occur early in the disease (Baloyannis, 2006). Despite such evidence, the mechanism of Golgi fragmentation in neurodegenerative diseases remains obscure. Because aberrant Cdk5 activity is present in several neurodegenerative diseases such as ALS, AD, and PD, we hypothesized that deregulated Cdk5 could be involved in Golgi disassembly in AD.

Cdk5 associates with Golgi to regulate membrane traffic under physiological conditions (Paglini *et al.*, 2001). However, it has not been linked to Golgi pathologically. Cdk5 belongs to the Cdk family of serine/threonine kinases, most of which play key regulatory roles in the progression of cell cycle (Beaudette *et al.*, 1993; Noble *et al.*, 2003). Although highly homologous to other members of the Cdk family, Cdk5 is not activated by cyclins. Instead, it is activated by specific regulatory binding partners, p35 or p39 (or their truncated forms, p25 and p29; Lew *et al.*, 1994; Tsai *et al.*, 1994, 2004; Lee *et al.*, 1996; Patrick *et al.*, 1999; Dhavan and Tsai, 2001; Cruz and Tsai, 2004). Although other Cdks are active in mitotic cells, Cdk5 was initially believed to be primarily active in postmitotic neurons. Cdk5's vital role in regulating various neuronal functions during embryogenesis and in adult brains has received broad acceptance (Ohshima *et al.*, 1996; Dhavan and Tsai, 2001; Ko *et al.*, 2001; Fischer *et al.*, 2003; Benavides and Bibb, 2004; Cruz and Tsai, 2004; Tsai *et al.*, 2004; Fischer *et al.*, 2005). Recent studies have revealed multiple extraneuronal roles of Cdk5 in various cell types (Rosales and Lee, 2006; Strock *et al.*, 2006; Goodyear and Sharma, 2007; Lin *et al.*, 2007).

This article was published online ahead of print in *MBC in Press* (http://www.molbiolcell.org/cgi/doi/10.1091/mbc.E07-11-1106) on May 14, 2008.

* These authors contributed equally to this work.

† Present address: Renovis, Inc., 2 Corporate Drive, South San Francisco, CA 94080.

Address correspondence to: Kavita Shah (shah23@purdue.edu).

Cdk5's kinase activity is tightly regulated by the spatial and temporal expression of p35 and p39. However, p35 and p39 are cleaved into p25 and p29 under a variety of pathological conditions such as oxidative stress, calcium dysregulation, Aβ exposure, excitotoxicity, inflammation and mitochondrial dysfunction in AD and PD (Patrick *et al.*, 1999; Lee *et al.*, 2000; Dhavan and Tsai, 2001; Strocchi *et al.*, 2003; Cruz and Tsai, 2004; Quintanilla *et al.*, 2004; Shea *et al.*, 2004; Tsai *et al.*, 2004; Kitazawa *et al.*, 2005; Qu *et al.*, 2007). Generation of p25 and p29 not only constitutively activates Cdk5, but also changes its subcellular localization from particulate to cytosolic and nuclear. This event allows Cdk5 to access a variety of pathological substrates, which triggers a cascade of neurotoxic pathways, ultimately causing neuronal death (Lau and Ahlijanian, 2003; Monaco, 2004; Smith *et al.*, 2004).

Cdk5/p25's role in NFT formation in AD has been well delineated (Liu *et al.*, 1995; Yamaguchi *et al.*, 1996; Pei *et al.*, 1998; Takahashi *et al.*, 2000; Augustinack *et al.*, 2002; Noble *et al.*, 2003). However, some studies support a more pivotal role of GSK3 (Plattner *et al.*, 2006), p38 and JNK in NFT formation. Moreover, it is not clear if tau hyperphosphorylation is enough to cause cell death. Nonetheless, Cdk5 deregulation can directly cause neuronal death independent of NFT formation. Transgenic mice expressing tetracycline inducible CamKII-p25 show significant brain atrophy, extensive astrogliosis, and NFT formation (Cruz *et al.*, 2003; Noble *et al.*, 2003). Deregulated p25/Cdk5 activity leads to aberrant APP processing, generating intracellular Aβ accumulation in vivo (Cruz *et al.*, 2006). Intracellular $A\beta_{1-42}$ has been detected in AD-vulnerable regions in human brains (Gouras *et al.*, 2000) and Tg animal models of AD (Oddo *et al.*, 2003; Casas *et al.*, 2004; Billings *et al.*, 2005; Cruz *et al.*, 2006) and is closely associated with neuronal loss (Casas *et al.*, 2004) and cognitive decline (Billings *et al.*, 2005). Oxidative stress can induce Cdk5-mediated cell death by either downregulating nestin scaffold (Sahlgren *et al.*, 2006) or nuclear MEF2 activity (Gong *et al.*, 2003). The mechanism of Cdk5-mediated cell death in AD, however, is not completely established. Because recent studies show that Golgi disassembly precedes neuronal cell death (Nakagomi *et al.*, 2008), the goal of this study was investigate if Cdk5 is involved in fragmenting Golgi.

β-Amyloid (Aβ) and glutamate are two primary neurotoxic stimuli in AD, and, hence, were chosen for this study. These stimuli activate Cdk5 by increasing intracellular levels of Ca^{2+} and reactive oxygen species (ROS; Patrick *et al.*, 1999; Shea *et al.*, 2004). However, their connection with Golgi fragmentation is not known. Cdk5 activity has not been linked to Golgi disassembly either. Our aim, therefore, was fourfold. Does Cdk5 promote Golgi disassembly downstream of Aβ and glutamate? Can Cdk5 initiate Golgi fragmentation, independent of other inputs? Is Golgi fragmentation alone sufficient to cause cell death? How does Golgi fragmentation occur via Cdk5? To pursue our first objective, we needed a Cdk5-specific inhibitor. Our second objective demanded an approach that specifically activates Cdk5 with high temporal control both in serum-starved and differentiated neuronal cells. Finally, the search for direct Cdk5 substrates could help in understanding Cdk5-mediated mechanism of Golgi fragmentation.

Cdk5's role has been mostly investigated by either constitutively expressing p25 or p35 or by using Cdk5-specific chemical inhibitors, such as roscovitine, the most widely used inhibitor to modulate Cdk5 activity (Meijer *et al.*, 1997; Gray *et al.*, 1999; Mapelli *et al.*, 2005). Both approaches have limitations. Overexpression of p25 or p35 lacks temporal control, which may be essential to uncover dynamic biological processes such as Golgi disassembly. Small molecule inhibitors of Cdk5 can provide high temporal control, but are not monospecific for Cdk5 (Meijer *et al.*, 1997; Sridhar *et al.*, 2006). Another problem with roscovitine from our perspective was its high affinity for Cdc2, a kinase that directly promotes Golgi fragmentation during mitosis. An ideal inhibitor should specifically target Cdk5, but not cross-react with Cdc2.

Cdk5 inhibitory peptide (CIP), a 126-residue artificial peptide containing $p35^{154-279}$, inhibits Cdk5 specifically and potently by blocking Cdk5/p25 complex formation, but not Cdk5/p35, when expressed endogenously (Amin *et al.*, 2002; Zheng *et al.*, 2002; Zheng *et al.*, 2005). CIP's affinity for Cdk5 is higher than p25's. However, as CIP needs to be overexpressed, this approach lacks temporal and dosage control.

To progress toward our objectives, novel tools to specifically activate and inhibit Cdk5 kinase activity in a highly temporal manner were required. To this end, we generated TAT-p25/TAT-p35 and TAT-CIP by fusing an 11-mer TAT sequence (residues 47–57 of HIV-Tat: YGRKKRRQRRR) to Cdk5-specific modulators (p25, p35, CIP). The first two specifically activate Cdk5 activity; the latter inhibits it. The fusion of TAT sequence, the minimal Tat transduction domain derived from human immunodeficiency virus 1 (HIV-1), results in efficient transduction into cells when directly added to cell culture or injected in vivo into mice (Nagahara *et al.*, 1998; Becker-Hapak *et al.*, 2001). These TAT-fusion proteins modulate Cdk5 activity in vitro and in various cell types (including primary neurons) with high temporal and dosage control. As our results showed that TAT-fusion proteins degrade in ~6 h in the cells, these tools provide an inducible control over Cdk5 activity. The versatility of these tools was demonstrated by maintaining inhibition of Cdk5 activity for 48 h during neuronal differentiation, which prevented neurite outgrowth. Cdk5 inhibition using TAT-CIP showed minimal effect on HT22 cell viability. In contrast, roscovitine was notably toxic, presumably due to the inhibition of Cdc2 and Cdk2.

With the aid of these novel genetic tools, we show that Cdk5 is responsible for Golgi fragmentation upon Aβ and glutamate stimulation in differentiated PC12 and SH-SY5Y cells, as well as in primary cortical neurons. Crucially, Cdk5 deregulation alone resulted in robust Golgi disassembly; however, this process alone is an insufficient trigger for cell death. A chemical genetic screen revealed *cis*-Golgi matrix protein GM130 as a novel substrate of Cdk5. Identification of Cdk5 phosphorylation site on GM130 suggested the mechanism by which Cdk5 may cause Golgi fragmentation upon deregulation in AD. As Cdk5 activity is deregulated in several neurodegenerative diseases where Golgi disassembly also occurs, we propose that Cdk5 may have a broader role beyond AD.

MATERIALS AND METHODS

Materials

Glutamate, poly-lysine, 3-(4,5-dimethyldiazol-2-yl)-2,5-diphenyltetrazolium bromide (MTT), and anti-FLAG antibody were obtained from Sigma (St. Louis, MO). β-amyloid$^{25-35}$ ($A\beta^{25-35}$) and 2′,7′-dichlorofluorescein diacetate (DCFDA) were purchased from Anaspec (San Jose, CA). Antibodies for Cdk5 (C-8), p35/p25 (C-19), actin (C-2), and GM130 (H-65) were purchased from Santa Cruz Biotechnology (Santa Cruz, CA). Antibody for phosphospecific GM130 was a gift from Martin Lowe. All transretinoic acid was purchased from Acros (Pittsburgh, PA), and roscovitine was obtained from LC Laboratories (Woburn, MA). Nerve growth factor (NGF) was obtained from Austral Biologicals (San Ramon, CA). Phalladoin-FITC, DAPI, FITC-goat anti-rabbit and Texas red goat anti-mouse antibodies were purchased from Molecular Probes (Eugene, OR).

Expression Plasmids and Constructs

Glutathione *S*-transferase (GST)-Cdk5 was a gift from Laurent Meijer. pET-28b-TAT (V2.1) and pTAT-HA vectors were gifts from Steve Dowdy. mPlum-RFP was a gift from Roger Tsein. p25, p35, CIP and mPlum-RFP (RFP) and GFP were cloned into pET-28b-TAT (V2.1) vector to generate TAT-fused proteins. TAT-fusion Peroxiredoxin-II (T89A) mutant [TAT-Prx-II (T89A)] was created using overlapping PCR in pTAT-HA vector. GM130 was cloned into pTAT-HA vector into BamHI and XhoI sites. TAT sequence was removed as a consequence of GM130 cloning into these sites.

Expression and Purification of GST-Cdk5 and TAT-Fusion Proteins

GST-Cdk5 was expressed and purified as described previously (Amin *et al.*, 2002). TAT-fusion proteins [TAT-p25, TAT-p35, TAT-CIP, TAT-RFP, TAT-GFP, GM130, and TAT-Prx-II (T89A)] were expressed in BL21 gold cells (Stratagene, La Jolla, CA). A single colony was inoculated into 50 ml of LB terrific broth liquid media with either 50 μg/ml kanamycin (TAT-p25, TAT-p35, TAT-CIP, TAT-RFP, and TAT-GFP) or 100 μg/ml ampicillin [TAT-Prx-II (T89A) and GM130] and was grown at 37°C overnight. This culture was added to 500 ml LB terrific broth. After it had grown to an OD ~ 0.6, protein synthesis was induced by the addition of IPTG (100 μM) and further shaking at 37°C for 6 h. After centrifugation at 5000 rpm for 15 min at 4°C, the cell pellet was frozen at −80°C for 1 h. The pellet was resuspended in chilled lysis buffer (20 mM Tris-HCl, pH 8.0, 150 mM NaCl, 1% NP-40, 10 mg/l aprotinin, 10 mg/l, 10 mg/l leupeptin, and 1 mM PMSF) and was French-pressed three times (Thermo Scientific, Waltham, MA). The resulting lysate was centrifuged at 10,000 rpm for 30 min at 4°C, and the supernatant was added to Ni-NTA beads and incubated at 4°C on a rotating wheel. The beads were washed five times by wash buffer (20 mM Tris-HCl, pH 8.0, 150 mM NaCl). The protein was eluted using 100 mM of imidazole in wash buffer. Protein concentration was determined using Bradford assay, and the protein purity was assessed by gel electrophoresis. All expressed TAT-fusion proteins were verified by Western blotting using 6-His antibodies.

Cell Culture

HT22 cells were a gift from David Schubert. HeLa and HT22 cells were cultured in DMEM supplemented with 10% fetal bovine serum (FBS). PC12 cells were grown in DMEM with 10% FBS and 5% horse serum. SH-SY5Y cells were cultured in DMEM plus 15% FBS.

Isolation of Primary Cortical Cells

Time pregnant CD1 mice and Sprague Dawley rats were purchased from Charles River (Wilmington, MA). Primary cortical neurons were isolated from E17 CD1 mice and Sprague Dawley rats embryos in Hanks' balanced salt solution. The tissue was minced, treated with 0.25 mg/ml trypsin, and dissociated by trituration in minimum essential media (MEM) supplemented with 130 U/ml DNase and 10% FBS. Cells were plated on poly-L-lysine–coated coverslips or plates in MEM supplemented with 5% FBS, 5% horse serum, 0.5 mM glutamine, 2.6 g/l glucose, 2.2 g/l $NaHCO_3$, and 1 mM pyruvate. Cultures were maintained at 37°C in a humidified 5% CO_2 atmosphere. All experiments were conducted on day 5.

Cdk5 Kinase Assay

Glutamate, $A\beta^{25-35}$, or TAT-fusion protein–treated cells were rinsed twice with cold PBS and lysed in 1% NP-40 lysis buffer (1% NP-40, 20 mM Tris, pH 8.0, 150 mM NaCl, 1 mM PMSF, 10 μg/ml leupeptin, and 10 μg/ml aprotinin) and cleared by centrifugation at 10,000 rpm for 10 min at 4°C. Cleared lysates were mixed with Cdk5 antibody and protein A Sepharose beads (Sigma) and incubated at 4°C for 2 h. Immune complexes were washed twice with 1% NP-40 lysis buffer and twice with kinase buffer (50 mM Tris, pH 8.0, 20 mM $MgCl_2$). Immune complexes were subjected to in vitro Cdk5 kinase assays using [γ-^{32}P]ATP and 5 μg of Cdk5 substrate peptide (KHHKSPKHR) in a final volume of 30 μl buffered at pH 8.0 containing 50 mM Tris and 20 mM $MgCl_2$ at 30°C. After 20 min, the reactions were terminated by spotting 25 μl of the reaction volume onto p81 phosphocellulose disks (Whatman, Clifton, NJ) and immersing in 100 ml of 10% acetic acid for 30 min, followed by three washings in 0.5% phosphoric acid (5 min each) and finally rinsing with acetone. The radioactivity was measured in a liquid scintillation counter.

Degradation Profile of TAT-Fusion Proteins

TAT-p25–treated HeLa cells and TAT-CIP–treated HT22 cells were harvested at indicated time points and lysed in 1% NP-40 buffer, respectively. TAT-p25/TAT-CIP was isolated from cell lysates using Ni-NTA beads for 1 h at 4°C. The beads were washed three times with wash buffer (20 mM Tris, pH 8.0, 150 mM NaCl), boiled in SDS loading buffer, and separated by electrophoresis. After transfer, the PVDF membrane was probed using 6-His antibody and the amount of TAT-p25/TAT-CIP was visualized using anti-mouse HRP in conjunction with West Pico (Pierce).

TAT-CIP Binding to Endogenous Cdk5

HT22 cells were lysed in 1% NP-40 buffer 45 min and 1 h after TAT-CIP addition. Cdk5 immune complexes were isolated for 4 h at 4°C. Beads were washed, proteins separated, transferred, probed with anti-6-His antibody, and visualized as described above.

ROS Measurement

For ROS measurement, 10^5 cells were seeded per well in a six-well plate in DMEM without phenol red. After 4-h treatment, DCFDA was added at a final concentration of 30 μM and incubated with cells for 20 additional min. Cells were detached by scraping gently and stored on ice. The fluorescence was measured immediately using a FACScalibur (BD Biosciences, San Jose, CA) with excitation wavelength of 488 nm and emission of 530 nm. Gated cells (n = 10,000) were analyzed for each sample.

PC12 Cells Differentiation

Cells were grown on poly-L-lysine–coated coverslips until 50–60% confluency, followed by serum starvation for 24 h. DMSO, roscovitine (10 μM), TAT-RFP (200 nM), or TAT-CIP (200 nM) were added 30 min before NGF (50 ng/ml) addition. For sustained treatment, TAT-fusion proteins were added every 6 h for 48 h. After incubating the cells for 48 h at 37°C, coverslips were washed three times with PBS, fixed in 3.7% Formalin/PBS for 10 min, and permeabilized with 0.1% Triton in PBS for 20 min. The cells were washed twice with PBS and blocked in 5% BSA/PBS for 1 h at 25°C. Cells were labeled with phalloidin fluorescein isothiocyanate (FITC; 800 ng/ml) and DAPI (1 μg/ml) for 1 h. Coverslips were mounted using Mowiol mounting media and neurite differentiation were scored using a Nikon E1000 fluorescence microscope (Melville, NY) equipped with a Retiga EXI cooled mono 12-bit camera, using a 20× objective. Two hundred cells were counted in each of five random fields, and cells bearing neurite extensions longer than twice the cell-body size were scored as differentiated cells.

MTT Assay

HT22 cells were seeded onto 12-well plates at 25,000 cells per well overnight, followed by DMSO, roscovitine (10 μM), TAT-RFP (200 nM), or TAT-CIP (200 nM) treatments. After 24 h, MTT was added to the final concentration of 0.5 mg/ml and incubated for 30 min. The cells were washed twice with PBS and lysed in dimethyl sulfoxide (DMSO), and the absorbance was measured at 570 nm. SH-SY5Y and PC12 cells were differentiated using NGF or retinoic acid for 3 d before the aforementioned treatments.

Immunofluorescence for Golgi Fragmentation

PC12 and SH-SY5Y cells were plated on poly-L-lysine–coated coverslips at a density of 12,000 cells per well in 24-well plates for 1 d. After 12 h of serum starvation, PC12 differentiation was induced using 50 ng/ml NGF for 3 d in DMEM supplemented with 0.5% FBS. SH-SY5Y cells were differentiated using 10 μM retinoic acid for 5 d in regular growth media. Differentiated cells and 5 d in vitro (DIV5) rat cortical cells were treated for 24 h with either 10 mM glutamate or 25 μM $A\beta^{25-35}$ together with either 200 nM TAT-CIP added every 4 h or 10 μM roscovitine. For the untreated samples, either 0.5 mM imidazole or 0.1% DMSO were used as controls for TAT-CIP and roscovitine, respectively. For TAT-p25 experiment 200 nM protein was added every 4 h, and 200 nM TAT- RFP was added as control. At the end of the treatment, media was aspirated and cells were fixed with chilled methanol for 5 min, rinsed with PBS, and incubated for 20 min with 5% BSA, 1% FBS, and 0.1% Triton X-100. An antibody against the Golgi resident enzyme mannosidase II was used: PC12 and primary cortical cells were immunostained using anti-mannosidase II from Covance Laboratories (Madison, WI; 1:3000). SH-SY5Y cells were stained with anti-mannosidase II from Chemicon (Temecula, CA; 1:100) for 2 h at room temperature. FITC-labeled goat anti-rabbit and Texas red–labeled goat anti-mouse antibodies were used at a 1:1000 dilution, together with DAPI (1 μg/ml). After three washes with PBS and one wash with water, coverslips were mounted on microscope slides with Mowiol mounting media. Images were taken using an E1000 Nikon fluorescence microscope equipped with a Retiga EXI cooled mono 12-bit camera using a 60× oil immersion objective. HeLa cells were plated for 12 h, serum-starved overnight, and treated with 100 μM $A\beta^{25-35}$ in the absence or presence of either 10 μM roscovitine, 200 nM TAT-CIP, or the controls: 0.5 mM imidazole or 0.1% DMSO. After 12 h of treatment, HeLa cells were fixed and processed in the same way as described for PC12 and SH-SY5Y cells and visualized in a confocal Nikon TE2000 inverted microscope with a Radiance Technologies 2100MP Rainbow Laser (Sunnyvale, CA). Percentage of cells with Golgi fragmentation was counted in at least 100 cells from 10 different frames, in triplicates. Cells with specific mannosidase II staining spread in the cytoplasm, with only a small amount of remaining juxtanuclear staining were scored as cells with fragmented Golgi.

Measurements from HeLa Confocal Images

Image J 1.36b software (Wayne Rasband, NIH; http://rsb.info.nih.gov/ij/) was used for the parameter quantification from the mannosidase II–stained

HeLa images. Perimeter of total cell area and Golgi area were manually selected and the number of pixels and intensity were scored. Area occupied by the intact Golgi or cluster of Golgi stacks (AOG parameter) was transformed to μm^2 according to the ratio 0.13 μm/pix, which corresponds to the magnification used for the imaging. To obtain a measurement of the dispersion, we measured the fluorescence per unit of area in the cytosol (CF/A): Golgi fluorescence was subtracted from the total cell fluorescence, and divided by the area of the cell excluding the Golgi. Background fluorescence measured from an area not occupied by cells was subtracted from this value to obtain the CF/A parameter. Percentage of fluorescence present in Golgi (% GFL) was obtained by dividing the fluorescence from the Golgi by the total cell fluorescence. These parameters were calculated on six representative cells from at least three random frames. Results are shown as the average with SE and *t* test significance; $^*p < 0.05$, $^{**}p < 0.01$.

Nuclear Staining Using Propidium Iodide

Differentiated PC12 and SH-SY5Y cells plated on coverslips were treated either with 10 mM glutamate or 25 μM $A\beta^{25-35}$ along with either 200 nM TAT-CIP added every 4 h or equal amount of TAT-GFP as a control. After the treatment, cells were fixed with cold methanol for 5 min, followed by rehydration in PBS and and permeabilization using 0.1% Triton X-100 in PBS plus 2% BSA. Cells were treated with 0.1 μg/ml RNase A in PBS for 1 h, rinsed, and stained with 2.5 μg/ml propidium iodide in PBS for 1 h. Before mounting with Mowiol, coverslips were washed twice with PBS and once with H_2O.

In Vitro Phosphorylation of GM130 by Cdk5/p25

HeLa cells were lysed in modified RIPA lysis buffer (50 mM Tris, pH 7.5, 150 mM NaCl, 1% NP-40, 0.25% sodium deoxycholate, 1 mM PMSF, 10 μg/ml leupeptin, and 10 μg/ml aprotinin) for 20 min on ice. After centrifugation, cell lysates was incubated with GM130 antibody (H-65, Santa Cruz) and protein Sepharose beads for 2.5 h at 4°C on a rotating wheel. The beads were washed twice with 1% NP-40 buffer and once with kinase buffer (20 mM $MgCl_2$, 20 mM Tris, pH 7.5). The beads were then incubated in a 30 μl reaction volume containing purified 6-His-Cdk5/p25 (isolated from SF9 cells), 10 mM Tris, pH 7.5, 20 mM $MgCl_2$, and 1 mM cold ATP for 1 h. The reaction mixture was separated on 10% SDS-PAGE, transferred to a PVDF membrane, and immunoblotted with Ser-25 phosphospecific GM130 antibody (gift from Martin Lowe). For loading control, the membrane was stripped with stripping solution (62.5 mM Tris, pH 6.8, 2% SDS and 100 μM 2-mercaptoethanol) at 60°C for 30 min and then washed with TBST extensively. The membrane was incubated overnight with 5% milk and probed with GM130 antibody, followed by HRP-linked secondary antibody.

p115 Binding Assay for GM130

GM130 was expressed in BL21 cells and purified using Ni-NTA beads. GM130 was phosphorylated using Cdk5/p25 complexes in vitro. p115 in pCMVTag2B vector was a gift from Dennis Shields. HeLa cells were transfected with p115 using the calcium phosphate method. After 36 h, cells were lysed using 1% NP-40 buffer, followed by immunoprecipation (IP) using anti-FLAG antibody. The beads were washed two times with 1% NP-40 buffer and once with kinase buffer. Unphosphorylated or phosphorylated GM130 was added to p115 beads and incubated at 4°C for 4 h. After washing, the binding of GM130 to p115 beads was detected by Western blot using 6-His antibody.

GM130 Phosphorylation and p115 Binding in HeLa Cells

HeLa cells were transfected with myc-GM130 using the calcium phosphate method. Serum starvation was started 12 h after transfection. 100 μM, Aβ, or 200 nM TAT-p25 was added and incubated for different times as indicated in the figure legends. At the end of treatment cells were rinsed with cold PBS, detached, and lysed in lysis buffer containing 1% NP-40, 50 mM Tris, 150 mM NaCl, 10% glycerol, 2 mM EDTA, 15 mM NaF, 1 mM PMSF, and 1 mM Na_3VO_4. Cleared lysates were loaded directly on SDS-PAGE gels or used for immunoprecipitation with 1 μg GM130 antibody and 5 μl protein A Sepharose. GM130 phosphorylation and p115 binding was probed using Western blot.

Statistical Significance

Bar graphs results are plotted as the average ± SEM. Significance was evaluated using Student's *t* test analysis and is displayed as follows: $^*p < 0.05$, $^{**}p < 0.01$, $^{***}p < 0.001$.

RESULTS

TAT-p25 Is a Temporal Activator of Cdk5 in Cell Lines and Primary Neurons

TAT-p25 was constructed by fusing TAT sequence with p25 for specific temporal activation of Cdk5, independent of other stimuli. TAT-RFP was generated as a control. An in vitro kinase assay was performed with increasing amount of TAT-p25 using GST-Cdk5 (50 nM). As shown in Figure 1A, maximal Cdk5 activation (set as 100%) was observed at ~500 nM TAT-p25 concentration. When equal concentration of TAT-RFP was incubated with GST-Cdk5, no change in Cdk5 activity was observed (data not shown).

TAT-p25 transduction in HeLa cells resulted in rapid activation of endogenous Cdk5 (~2.5-fold), which can be controlled by modulating TAT-p25 levels (Figure 1B). No Cdk5 activation was observed, when TAT-RFP was added (data not shown). Previous studies have recommended adding ~50–300 nM TAT-fusion proteins to the cells to dissect biological functions (Nagahara *et al.*, 1998; Becker-Hapak *et al.*, 2001). We consistently observed maximal Cdk5 activation at ~200 nM TAT-p25 in several independent experiments. However, when a large excess of TAT-p25 was added (usually >300 nM), less Cdk5 activation was observed. Presumably, at a higher concentration TAT-protein interacts with other serum proteins, causing aggregation, and thus sufficient protein may not get inside the cells (Becker-Hapak and Dowdy, 2003). To further confirm if TAT-p25 activates Cdk5 maximally at 200 nM concentrations, HeLa cells were transfected with p25, and Cdk5 activation was measured. Cdk5 activation increased 2.5-fold upon p25 overexpression (Figure 1, C and D), suggesting that TAT-p25 transduction and p25 overexpression activate Cdk5 to comparable levels. Similar results were obtained when TAT-p25 was transduced in primary cortical neurons isolated from mouse embryos (Figure 1E). TAT-RFP transduction showed no effect on Cdk5 activity (Figure 1E). As Cdk5 plays a key role in neurodegenerative diseases, this tool should be particularly useful in dissecting Cdk5's function in neurons.

TAT-p25 Activates Endogenous Cdk5 with Inducible Temporal Control

A potential advantage of TAT-p25–mediated transduction is to have inducible control over endogenous Cdk5 activity, as exogenously added proteins should degrade over time inside the cells. We conducted a time course of TAT-p25–induced Cdk5 activation (measured up to 6 h). TAT-p25 was isolated from TAT-p25–treated HeLa cells at different times after transduction. As shown in Figure 1F, the highest concentration of TAT-p25 was observed at 1 h, which slowly returns to basal levels in 6 h. As TAT-p25–mediated activation of Cdk5 wanes after 4 h, it confirms the same conclusion (Figure 1G). This important feature can be used for transient activation of Cdk5. Alternatively, if sustained Cdk5 activation is required, TAT-p25 can be added every 4–6 h.

TAT-p35 Is a Temporal Activator of Cdk5

TAT-p35 was generated and used to activate GST-Cdk5 in vitro. Similar to TAT-p25, TAT-p35 activated Cdk5 in a dose-dependent manner (Figure 1H); however, the maximum Cdk5 activation by TAT-p35 was only ~80% of the maximum Cdk5 activation by TAT-p25 (cf. Figure 1, A and H). TAT-p35 was next transduced in HeLa cells, and Cdk5 kinase activity was evaluated (Figure 1I). The maximal endogenous Cdk5 activation by TAT-p35 was ~1.5-fold compared with p25-mediated activation, which was ~2.5-fold (compare Figure 1, B and I). This result was expected as p35-mediated Cdk5 activation is lower than p25-mediated activation in vitro (cf. Figure 1, A and B; Amin *et al.*, 2002).

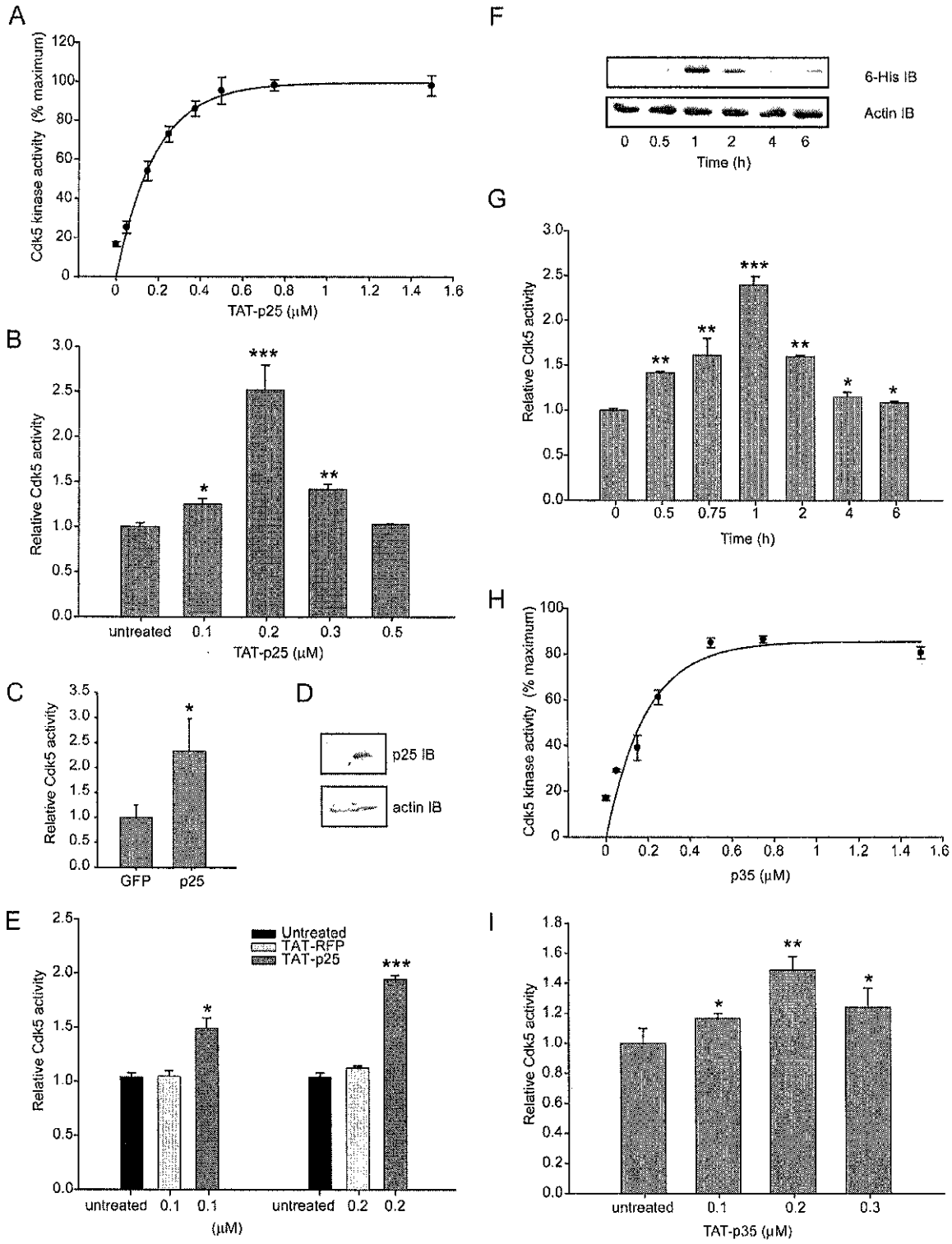

Figure 1. TAT-p25 and TAT-p35 are inducible Cdk5 activators in vitro and in the cells. (A) Activation of Cdk5 as a function of TAT-p25 concentration in vitro. The reaction mixtures containing 50 nM GST-Cdk5 and the indicated amounts of TAT-p25 were incubated at 30°C for 30 min, followed by kinase assays as described in *Materials and Methods*. One hundred percent of Cdk5 activation represents the maximum activation of Cdk5 by TAT-p25. All values are significantly above baseline ($p < 0.0001$). (B) Transduction of TAT-p25 activates endogenous Cdk5 in HeLa cells. Cells ($n = 10^6$) were seeded onto 100-mm plates overnight. Indicated amounts of TAT-p25 were incubated with cells for 1 h. Cdk5 was immunoprecipated, followed by kinase assays. (C) HeLa cells were transfected with GFP or p25. After 24 h, Cdk5 was immunoprecipitated, and its kinase activity was assayed. (D) Transfection efficiency of p25 was evaluated by Western blot using p35 antibody

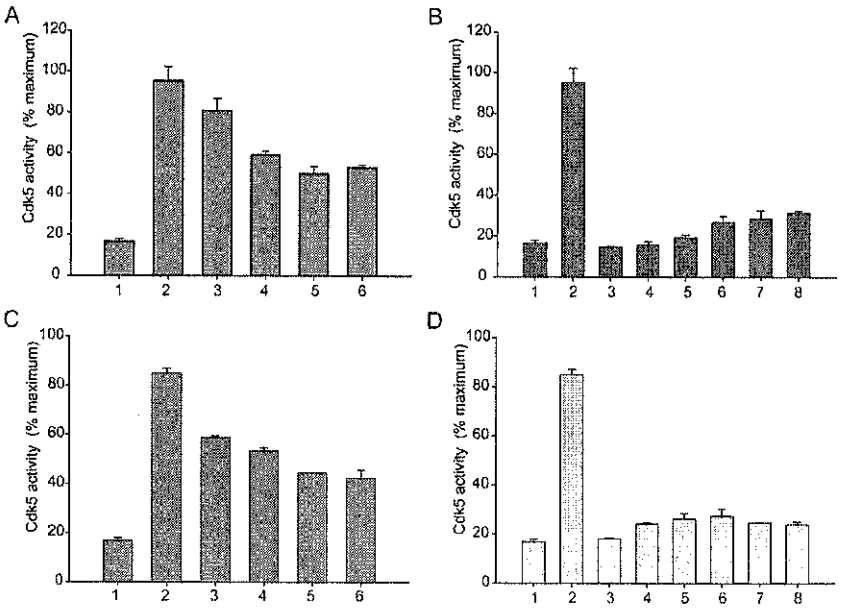

Figure 2. TAT-CIP prevents Cdk5 activation by p25 or p35 when added before Cdk5/p25 or Cdk5/p35 complex formation in vitro. (A) TAT-CIP is inefficient in inhibiting Cdk5 activity in TAT-p25/Cdk5 preformed complexes in vitro. For maximum activation of Cdk5 by p25 (set as 100%), 50 nM GST-Cdk5 and 500 nM TAT-p25 were preincubated at 30°C for 30 min according to Figure 1A. Next, increasing amounts of TAT-CIP were added and incubated at 30°C for additional 30 min, followed by kinase assays. Column 1, Cdk5; 2, Cdk5/p25 (set as 100%); 3, Cdk5/p25 + 100 nM TAT-CIP; 4, Cdk5/p25 + 250 nM TAT-CIP; 5, Cdk5/p25 + 500 nM TAT-CIP; 6, Cdk5/p25 + 1 μM TAT-CIP. (B) For maximal Cdk5 inhibition by CIP, 50 nM GST-Cdk5 and 500 nM TAT-CIP were preincubated at 30°C for 30 min to form the complexes according to Figure 2A. Next, increasing amounts of TAT-p25 were added and incubated for additional 30 min, followed by kinase assays. Column 1, Cdk5; 2, Cdk5/p25 (set as 100%); 3, Cdk5/CIP; 4, Cdk5/CIP + 100 nM TAT-p25; 5, Cdk5/CIP + 250 nM TAT-p25; 6, Cdk5/CIP + 375 nM TAT-p25; 7, Cdk5/CIP + 500 nM TAT-p25; 8, Cdk5/CIP + 1.5 μM TAT-p25. (C) TAT-CIP is inefficient in inhibiting Cdk5 activity in TAT-p35/Cdk5 preformed complexes in vitro. For maximum activation of Cdk5 by p35, 50 nM GST-Cdk5 and 500 nM TAT-p35 were preincubated at 30°C for 30 min according to Figure 1H. Next, increasing amounts of TAT-CIP were added and incubated at 30°C for additional 30 min, followed by kinase assays. Column 1, Cdk5; 2, Cdk5/p35 (100% represents maximum activity of Cdk5/p25); 3, Cdk5/p35 + 100 nM TAT-CIP; 4, Cdk5/p35 + 250 nM TAT-CIP; 5, Cdk5/p35 + 500 nM TAT-CIP; 6, Cdk5/p35 + 1 μM TAT-CIP. (D) For maximal Cdk5 inhibition by CIP, 50 nM GST-Cdk5 and 500 nM TAT-CIP were preincubated at 30°C for 30 min to form the complexes according to 2C. Next, increasing amounts of TAT-p35 were added and incubated for additional 30 min, followed by kinase assays. Column 1, Cdk5; 2, Cdk5/p35; 3, Cdk5/CIP; 4, Cdk5/CIP + 100 nM TAT-p35; 5, Cdk5/CIP + 250 nM TAT-p35; 6, Cdk5/CIP + 375 nM TAT-p35; 7, Cdk5/CIP + 500 nM TAT-p35; 8, Cdk5/CIP + 1.5 μM TAT-p35. All the data shown are mean ± SEM.

TAT-CIP Is a Specific Inhibitor of Cdk5 with High Temporal Control

Although TAT-p25 and TAT-p35 provide effective ways to isolate the sole consequences of Cdk5 activation in a temporal manner, they do not allow isolating specific Cdk5 functions downstream of various stimuli. Because CIP peptide is specific for Cdk5 (Amin *et al.*, 2002; Zheng *et al.*, 2002, 2005), it was chosen to develop a specific Cdk5 inhibitor. To encode the temporal control feature in CIP, TAT-fusion CIP was generated.

TAT-CIP Prevents Cdk5 Activation by p25 In Vitro

An earlier study showed that CIP can bind to Cdk5 and inhibit its activity to basal levels in vitro, but not when it is in preformed complex with p16, the minimum active truncated peptide of p35 (Amin *et al.*, 2002). However, all the proteins used in that study were GST-tagged, which could cause artifacts due to GST dimerization. Furthermore, it has been shown that CIP transfection inhibits Cdk5 activity in the cells (Zheng *et al.*, 2002, 2005), which could occur either by breaking the Cdk5/p25 complex or by preventing p25 from binding/activating Cdk5.

In our study, although Cdk5 was expressed as a GST-tagged protein, both TAT-p25 and TAT-CIP were generated as 6-His tagged. Increasing amounts of TAT-CIP were added to the preformed Cdk5/p25 complex that had maximum Cdk5 activity (set as 100%) according to Figure 1A, and Cdk5 activity was measured. Similar to results reported earlier (Amin *et al.*, 2002), TAT-CIP could only decrease Cdk5 activity by ~50% when added to the Cdk5/p25 preformed complex (Figure 2A). However, when TAT-CIP was added to Cdk5 before p25, it prevented p25 activation of Cdk5 (Figure 2B). Only slight increase in Cdk5 activity was observed when a large excess of p25 was added to the Cdk5/CIP complex. This result suggests that TAT-CIP could protect the cells from Cdk5-mediated toxicity when added before the neurotoxin or any other toxic stimulation.

Figure 1 (cont). and anti-actin antibody as loading control. (E) Transduction of TAT-p25 activates endogenous Cdk5 in primary cortical neurons. Primary cortical neurons were isolated from E17 CD-1 mouse embryos and seeded onto 100-mm plates for at least 4 d. Indicated amounts of TAT-p25 or TAT-RFP were incubated with cells for 1 h. Cdk5 IP and kinase assays were conducted. (F) TAT-p25 is degraded over time in the cells. TAT-p25 was isolated by Ni-NTA beads from TAT-p25–treated HeLa cells at indicated times, separated by SDS-PAGE, and transferred to PVDF membrane. TAT-p25 was visualized using 6-His antibody (top panel). Ten percent of the whole cell lysate was used as a loading control and immunoblotted using actin antibody (bottom panel). (G) Time course of Cdk5 activation in HeLa cells induced by TAT-p25. TAT-p25 at 200 nM was incubated with cells at indicated times. Cdk5 IP and kinase assays were conducted. (H) Activation of Cdk5 as a function of TAT-p35 concentration in vitro. The reaction mixtures containing 50 nM GST-Cdk5 and the indicated amounts of TAT-p35 were incubated at 30°C for 30 min, followed by kinase assays. One hundred percent of Cdk5 activation represents the maximum activation of Cdk5 by TAT-p25 shown in A. All values are significantly above baseline ($p < 0.0001$). (I) Transduction of TAT-p35 activates endogenous Cdk5 in HeLa cells. Indicated amounts of TAT-p35 were incubated with cells for 1 h. Cdk5 IP and kinase assays were conducted. All the data shown are mean ± SEM; *$p < 0.05$; **$p < 0.01$; ***$p < 0.001$ compared with untreated sample.

TAT-CIP Prevents p35 Activation of Cdk5 In Vitro

We next investigated if TAT-CIP can inhibit Cdk5/p35 complex formation. Addition of TAT-CIP in the presence of the Cdk5/p35 preformed complex led to maximum inhibition of ~50% (Figure 2C), similar to the results obtained using p25 (Figure 2A). Interestingly, a previous study showed that CIP is unable to inhibit the Cdk5/p35 complex when expressed endogenously (Zheng *et al.*, 2002, 2005); in contrast, our results revealed that TAT-CIP efficiently prevents p35 activation of Cdk5, when added before Cdk5/p35 complex formation (Figure 2D).

TAT-CIP Inhibits Cdk5 Activity upon Glutamate Stimulation in HT22 Cells

Because glutamate activates Cdk5 activity in neuronal cells, HT22 cells (immortalized mouse hippocampal cells) were chosen to investigate Cdk5's role on glutamate stimulation. HT22 cells do not respond to excitotoxicity upon glutamate stimulation. Instead, they respond to extracellular glutamate by oxytosis, which prevents cystine uptake, resulting in glutathione loss in the cells. As glutamate concentration varies from 1 to 10 mM in the synaptic cleft and intraneuronal compartments (Dzubay and Jahr, 1999), the Cdk5 activation profile was monitored at 10 μM and 5 mM concentration. Cdk5 was activated at both concentrations (see Figure 3, A and B). However, the peak activation, after 10 μM and 5 mM glutamate treatment, was observed at 60 and 30 min, respectively (data not shown).

TAT-CIP was added to HT22 cells upon 10 μM glutamate stimulation at t = 0, and Cdk5 activity was measured after 1 h. Glutamate at 10 μM activates Cdk5 more than twofold within 1 h, which was inhibited by TAT-CIP (Figure 3A). Importantly, TAT-CIP was added at the same time as glutamate in these experiments, suggesting that TAT-CIP can inhibit Cdk5 activity to basal levels if added at the time of stimulation by preventing Cdk5/p25 complex formation (Figure 3A).

Similar results were obtained when HT22 cells were treated with 5 mM glutamate, and Cdk5 activity was measured after 30 min (Figure 3B). As maximal Cdk5 activation is relatively more rapid at 5 mM glutamate than at 10 μM (30 min vs. 1 h), TAT-CIP needs to be added 30 min before stimulation for maximal Cdk5 inhibition.

TAT-CIP Inhibits Cdk5 Activity in Primary Neurons upon $A\beta^{25-35}$ Stimulation

Multiple studies have documented Cdk5 activation upon Aβ stimulation due to cleavage of p35 to p25 (Patrick *et al.*, 1999; Dhavan and Tsai, 2001; Cruz and Tsai, 2004; Tsai *et al.*, 2004). In this study, we used $A\beta^{25-35}$, which is the biologically active and highly toxic core fragment of full-length Aβ ($A\beta^{1-42}$; Yankner *et al.*, 1990; Pike *et al.*, 1995). $A\beta^{25-35}$ is produced by enzymatic cleavage of naturally occurring Aβ in brains of AD patients (Kubo *et al.*, 2002). Previous studies have shown that acute icv administration of $A\beta^{25-35}$ induces the deposition of endogenously produced amyloid protein. In addition, $A\beta^{25-35}$ induces neurotoxic effects similar to those produced by $A\beta^{1-42}$ and generates neuropathological signs related to those of early stages of AD (Maurice *et al.*, 1998; Stepanichev *et al.*, 2003; Cheng *et al.*, 2006; Klementiev *et al.*, 2007).

When TAT-fusion proteins were added to $A\beta^{25-35}$-treated primary cortical neurons, TAT-RFP showed no effect (Figure 3C). However, TAT-CIP addition 30 min before $A\beta^{25-35}$ stimulation resulted in complete inhibition of Cdk5 activity (Figure 3C). This result confirms that TAT-CIP inhibits Cdk5 activity to basal levels in a highly temporal manner in primary neurons by preventing Cdk5 from binding to p25 formed upon neurotoxic stimulation.

TAT-CIP Specifically Binds Cdk5 in the Cells

To further ensure that TAT-CIP–mediated inhibition of Cdk5 activity was due to its specific binding, Cdk5 immune complexes were isolated from TAT-CIP–treated cells and probed using 6-His antibody. As shown in Figure 3D, TAT-CIP specifically binds Cdk5 inside the cells.

TAT-CIP Provides Inducible Control over Cdk5 Activity

Similar to TAT-p25, TAT-CIP was expected to degrade over time in the cells. TAT-CIP was isolated from TAT-CIP–treated HT22 cells at different times after transduction. As shown in Figure 3E, the highest concentration of TAT-CIP was observed at 1 h, which degraded to background levels in 6 h after addition to HT22 cells. This property of TAT-fusion proteins can be used to examine Cdk5's role in a pathway by specifically inducing either transient or sustained inhibition (or activation) of Cdk5.

Examination of Possible Toxicity Induced by TAT-Fusion Proteins

The strategy of TAT-mediated protein transduction has been used extensively in recent years for studying signal transduction. Because both CIP and p25 are small proteins, their transduction was very efficient. However, there are two main concerns with TAT-transduction studies. First, TAT-fusion proteins often employ the endosomal pathway, resulting in improper destination, which renders them nonfunctional (Shiraishi *et al.*, 2005). Second, as TAT is derived from HIV, cytotoxicity is a concern. Recent studies have documented that the HIV protein Tat induces neurotoxicity and oxidative stress both directly and indirectly (Pocernich *et al.*, 2005). Although we used TAT-peptide (residues 47–57 of HIV-Tat: YGRKKRRQRRR) instead of Tat, both concerns were addressed in this study.

Previous studies have shown that cationic peptides like TAT-fusion proteins predominantly enter via the endosomal pathway, which can be released using either 6 mM Ca^{2+} or lysosomotrophic agents such as chloroquine (Shiraishi *et al.*, 2005). However, in that study, a large excess of TAT-fusion proteins (0.5–4 μM) was used compared with the amount in the present study (200 nM), which may contribute to toxicity. Nevertheless, to elucidate if TAT-p25 transduction was mediated by the endosomal pathway, TAT-p25–treated cells were further treated with either $CaCl_2$ (1–10 mM) or chloroquine, both of which facilitate endosomal release. Neither $CaCl_2$ nor chloroquine showed any increase in Cdk5 activation (data not shown), implying that either sufficient TAT-p25 is able to bind Cdk5 independent of the endosomal pathway or that TAT-p25 transduction is not predominantly due to endocytosis. However, addition of excess TAT-fusion protein may lead to transduction via the endosomal pathway.

Because full-length HIV-Tat can cause ROS formation, we next examined a possible role for TAT-fusion protein in inducing oxidative stress. Peroxiredoxin-II (T89A) [(Prx-II (T89A)] mutant protein was cloned as the corresponding TAT-fusion protein. Prx-II is a major antioxidant protein that is responsible for eliminating ROS in the cytosol (Kang *et al.*, 2005). Because Prx-II activity is eliminated upon phosphorylation, we generated Prx-II (T89A), which is resistant to phosphorylation (Chang *et al.*, 2002; Jang *et al.*, 2006). This step eliminates any artifact that may be caused upon post-translational modification in the cells.

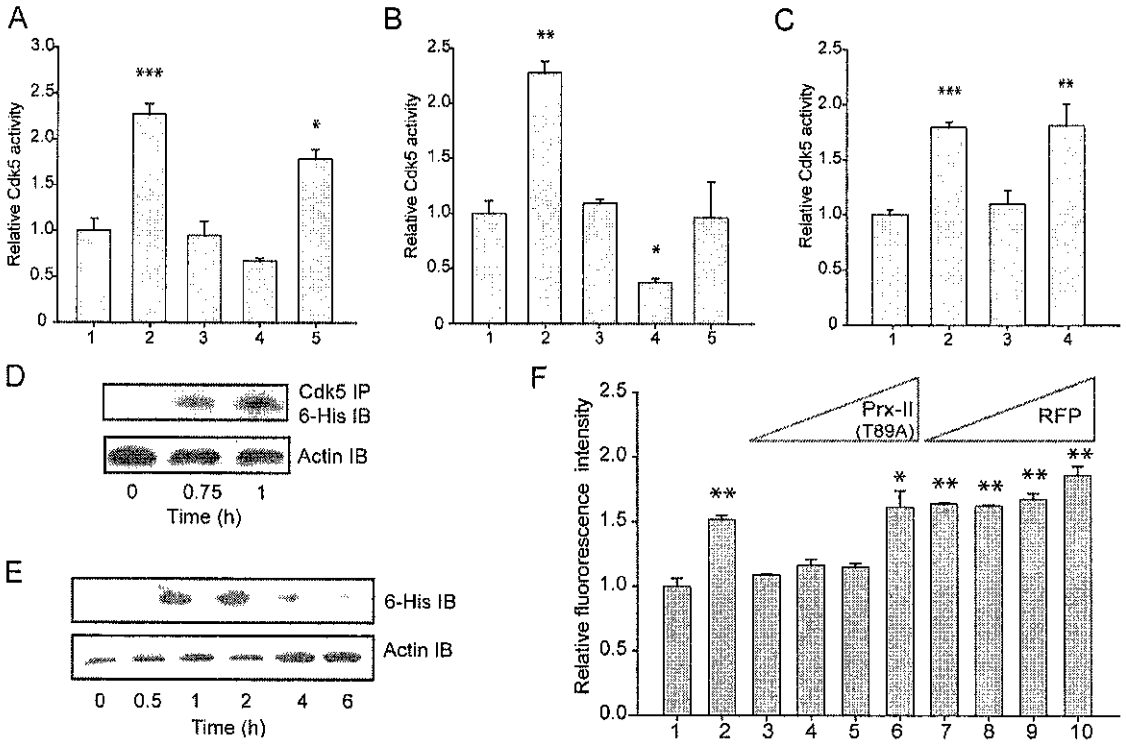

Figure 3. TAT-CIP binds and inhibits endogenous Cdk5 specifically upon neurotoxic stimulation in the cells. (A) TAT-CIP inactivates endogenous Cdk5 in HT22 cells stimulated with 10 μM of glutamate. Cells (n = 10^6) were seeded on 100-mm plates overnight. Indicated amounts of TAT-CIP and 10 μM glutamate were added simultaneously. After 1-h incubation, Cdk5 IP and kinase assay were conducted. Column 1, no treatment; 2, glutamate; 3, glutamate + 100 nM TAT-CIP; 4, glutamate + 200 nM TAT-CIP; 5, glutamate + 500 nM TAT-CIP. (B) TAT-CIP inactivates endogenous Cdk5 in HT22 cells stimulated with 5 mM of glutamate. Indicated amounts of TAT-CIP were added 30 min before 5 mM glutamate. After 30 min of glutamate stimulation, Cdk5 IP and kinase assay were conducted. Column 1, no treatment; 2, glutamate; 3, 100 nM TAT-CIP + glutamate; 4, 200 nM TAT-CIP + glutamate; 5, 500 nM TAT-CIP + glutamate. (C) Transduction of TAT-CIP inactivates endogenous Cdk5 in primary cortical neurons upon $A\beta^{25-35}$ stimulation. TAT-CIP at 200 nM was added to primary cortical neurons 30 min before stimulation of 20 μM $A\beta^{25-35}$. TAT-RFP at 200 nM was used as control. After additional 30 min of $A\beta^{25-35}$ stimulation, Cdk5 IP and kinase assay were conducted. Column 1, no treatment; 2, $A\beta^{25-35}$; 3, TAT-CIP + $A\beta^{25-35}$; 4, TAT-RFP + $A\beta^{25-35}$. All the data shown are mean ± SEM. (D) TAT-CIP binds to endogenous Cdk5 in the cells. After TAT-CIP was added to the HT22 cells for indicated times, Cdk5 immune complexes were isolated, separated by SDS-PAGE, and transferred to PVDF membrane. TAT-CIP was immunodetected using 6-His antibody (top panel). Ten percent of the whole cell lysate was used as a loading control and immunoblotted using actin antibody (bottom panel). (E) TAT-CIP is degraded over time after addition to the culture. TAT-CIP was isolated by Ni-NTA beads from TAT-CIP–treated HT22 cells at indicated times, separated by SDS-PAGE, and transferred to PVDF membrane. TAT-CIP was immunodetected using 6-His antibody (top panel). Ten percent of the whole cell lysate was used as a loading control and immunoblotted using actin antibody (bottom panel). (F) TAT-Prx-II (T89A) reduces ROS formation upon 5 mM glutamate stimulation in HT22 cells. Indicated amounts of either TAT-Prx-II (T89A) or TAT-RFP were added to HT22 cells, followed by 5 mM glutamate stimulation. After 4-h incubation, DCFDA staining was conducted as described in *Materials and Methods*. Column 1, no treatment; 2, glutamate; 3, 50 nM TAT-Prx-II (T89A) + glutamate; 4, 100 nM TAT-Prx-II (T89A) + glutamate; 5, 200 nM TAT-Prx-II (T89A) + glutamate; 6, 500 nM TAT-Prx-II (T89A) + glutamate; 7, 50 nM TAT-RFP + glutamate; 8, 100 nM TAT-RFP + glutamate; 9, 200 nM TAT-RFP + glutamate; 10, 500 nM TAT-RFP + glutamate. All the data shown are mean ± SEM.

For ROS measurement using DCFDA staining, fluorescence was recorded at an excitation wavelength of 488 nm and an emission wavelength of 530 nm. To avoid overlap at these wavelengths, TAT-RFP was used as a negative control. mPlum-RFP emits at 649 nm, and thus is the farthest-red emitter identified so far (Shaner *et al.*, 2005). As mentioned above, preliminary experiments using TAT-RFP revealed neither toxicity nor Cdk5 activation in HT22 (data not shown) and primary cortical cells (Figures 1E and 3C).

To induce ROS formation, HT22 cells were stimulated using glutamate (5 mM), and ROS levels were evaluated using DCFDA staining via flow cytometry (Stanciu *et al.*, 2000). Although addition of TAT-Prx-II (T89A) with optimized concentration (50–200 nM) to HT22 cells eliminated ROS upon glutamate stimulation, TAT-RFP showed no effect (Figure 3F). These results suggest that TAT-fusion proteins may not cause ROS formation unless added at very high concentrations. TAT-Prx-II (T89A)-mediated elimination of ROS presents another example of an active TAT-fusion enzyme, which can be used in a highly temporal and dose-dependent manner.

TAT-CIP Reduces Cell Differentiation upon NGF Stimulation

We next wanted to investigate if TAT-fusion proteins could be used for prolonged modulation of Cdk5 activity without causing any toxicity. Because differentiated PC12 cells are well-studied models for isolating Cdk5 contribution, these cells were chosen. Previous studies have shown that Cdk5 is inactive in dividing neuronal cells. It becomes progressively more active in differentiating cells (Yan and Ziff, 1995; Harada *et al.*, 2001) and is predominantly expressed in ter-

minally differentiated neurons (Lew *et al.*, 1994; Tsai *et al.*, 1994; Dhavan and Tsai, 2001). NGF treatment triggers PC12 cells differentiation into sympathetic-like neurons, which is characterized by neurite outgrowth (Greene and Tischler, 1976; Marshall, 1995; Harada *et al.*, 2001; Li *et al.*, 2007). Cdk5/p35 complex is essential for neurite outgrowth (Nikolic *et al.*, 1996; Xiong *et al.*, 1997; Paglini *et al.*, 1998). Disruption of either of the genes that encode these proteins leads to defects in neuronal migration and cortical lamination in mice (Ohshima *et al.*, 1996; Chae *et al.*, 1997). The expression of p35, and thus the kinase activity of Cdk5, is strongly induced by NGF stimulation. Inhibition of Cdk5 by roscovitine blocks NGF-induced neurite outgrowth (Harada *et al.*, 2001).

PC12 cells were serum-starved for 24 h, followed by NGF treatment (50 ng/ml) up to 48 h. To assess Cdk5's contribution, PC12 cells were treated with either roscovitine (10 μM) or TAT-CIP (200 nM), 30 min before NGF stimulation. TAT-CIP was either added once or every 6 h (sustained). TAT-RFP was used as a control. Although TAT-CIP efficiently inhibited neurite outgrowth, TAT-RFP showed no effect (Figure 4, A and B). Thus, TAT-CIP can be used for both transient and sustained inhibition of Cdk5 activity.

In addition, although previous studies have shown that CIP does not inhibit Cdk5/p35 in the cells (Zheng *et al.*, 2002, 2005), our results show that TAT-CIP can inhibit Cdk5/p35 complex formation both in vitro (Figure 2D) and inside the cells (Figure 4, A and B) if added before Cdk5/p35 complex formation. As neurite outgrowth is due to Cdk5/p35 activity, TAT-CIP–mediated inhibition of neurite outgrowth further confirms that TAT-CIP can prevent Cdk5 from binding of endogenous p35 upon NGF stimulation. Reduction in neurite outgrowth observed upon transient addition of TAT-CIP after NGF stimulation further supports this conclusion.

Cdk5 Inhibition Using TAT-CIP Shows Minimal Effect on Cell Viability

As noted earlier, roscovitine inhibits both Cdc2 and Cdk2 (Meijer *et al.*, 1997), which should result in cell death irrespective of Cdk5. Several studies support Cdk5's role in cell differentiation, proliferation, or survival in various cell types using roscovitine (Harada *et al.*, 2001; Sharma *et al.*, 2004; Goodyear and Sharma, 2007; Zheng *et al.*, 2007). The key advantage of using TAT-CIP compared with other pharmacological inhibitors of Cdk5 is its ability to isolate the consequences of Cdk5 activity solely in the presence of other Cdks.

An MTT assay was conducted to assess cell viability of HT22 cells subjected to either 10 μM roscovitine or TAT-CIP (transient and sustained addition) for 24 h, which allows completion of at least one cell cycle. Although roscovitine treatment curtailed cell viability by 50% in 24 h, both transient and sustained addition of TAT-CIP showed minimal effect (Figure 4C). Reduced cell viability upon roscovitine

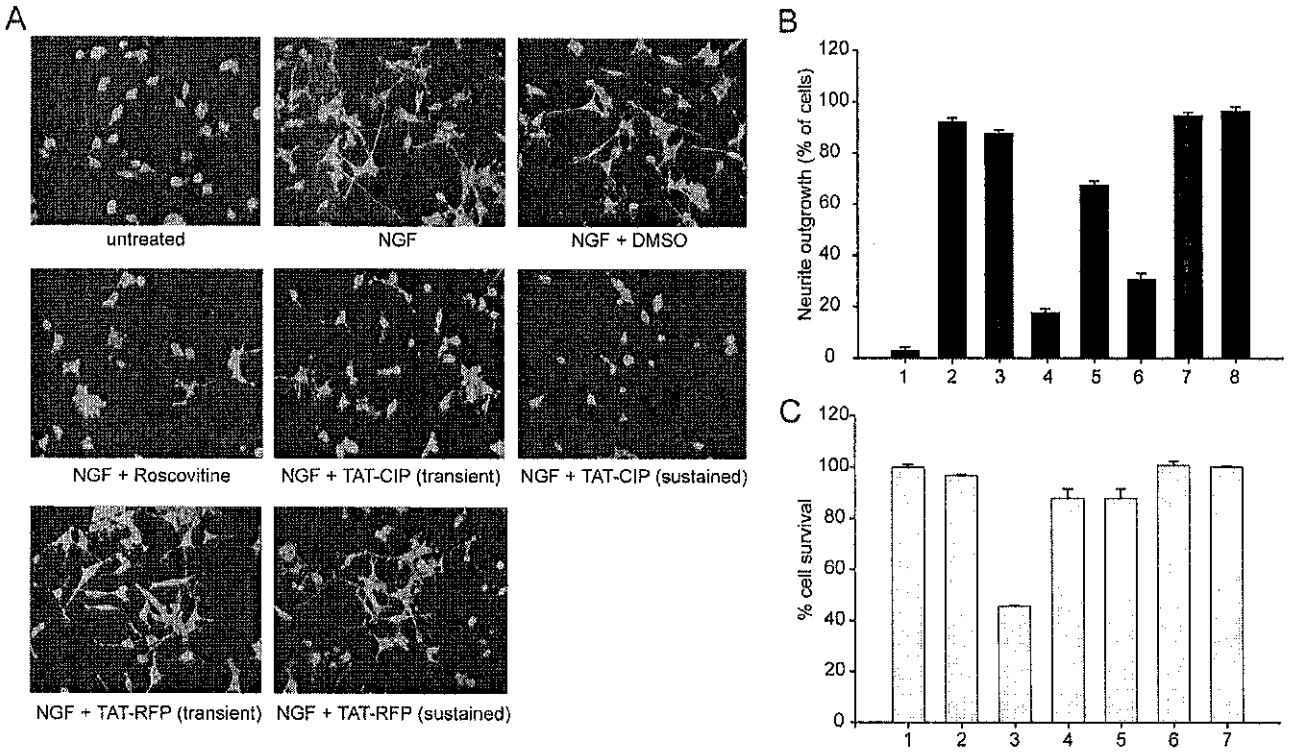

Figure 4. Consequences of Cdk5 activity can be isolated using transient or sustained TAT-CIP addition with minimal toxicity. (A and B) Inhibition of Cdk5 by TAT-CIP reduces neurite outgrowth in PC12 cells upon NGF stimulation. PC12 cells were serum-starved for 24 h, followed by 50 ng/ml NGF stimulation plus treatments as indicated for 48 h. (A) Images show the distribution of nuclei and F-actin staining as described in *Materials and Methods*. (B) The percentage of neurite outgrowth: column 1, no treatment; 2, NGF; 3, DMSO + NGF; 4, 10 μM roscovitine + NGF; 5, transient TAT-CIP addition + NGF; 6, sustained TAT-CIP addition + NGF; 7, transient TAT-RFP addition + NGF; 8, sustained TAT-RFP addition + NGF. (C) Although roscovitine arrests the cells presumably by blocking Cdc2 and Cdk2, TAT-CIP is specific for Cdk5 and is not toxic to the cells. HT22 cells were seeded 25,000 cells per well in 12-well plates overnight, followed by treatments as indicated for 24 h. MTT assay was performed as described in *Materials and Methods*. Column 1, no treatment; 2, DMSO; 3, 10 μM roscovitine; 4, transient addition of TAT-CIP; 5, sustained addition of TAT-CIP; 6, transient addition of TAT-RFP; 7, sustained addition of TAT-RFP. All the data shown are mean ± SEM.

treatment was presumably due to inhibition of Cdc2 for a prolonged period. Because TAT-CIP efficiently prevented neurite formation upon NGF stimulation (Figure 4, A and B), but did not affect cell viability, it suggests that Cdk5 inhibition is not toxic in HT22 cells, contrary to the results obtained using roscovitine (Figure 4C).

TAT-CIP Rescues Golgi Fragmentation in HeLa Cells Induced by $A\beta^{25-35}$

Having established the validity of these novel tools, we proceeded to evaluate Cdk5's role in Golgi fragmentation. To examine the morphology of fragmented Golgi at high resolution, HeLa cells were initially chosen for their relatively large size and flat-adherent phenotype. A direct link between Aβ and Golgi morphology has not been delineated in any cell type. Our initial goal was to investigate if Aβ treatment could promote Golgi disassembly. To eliminate Golgi fragmentation during mitosis, these cells were starved for 12 h in serum-free media, followed by 100 μM $A\beta^{25-35}$ treatment for 12 h. Golgi morphology was evaluated using mannosidase II. In control cells, Golgi can be seen in two morphologies: Golgi ribbon that represents a 17.8 ± 1.8% of total number of cells (§ in Figure 5, A and B) or a round accumulation of short ministacks: 77 ± 1.5% of total number of cells (# in Figure 5, A and B). Confocal pictures showed that Golgi ribbon measures 16 ± 3 μm in length, 1 ± 0.3 μm thickness, whereas round Golgi (#) has a diameter of 5 ± 2 μm. In contrast, in $A\beta^{25-35}$-treated cells, only 5.9 ± 1.4% of cells have a Golgi ribbon, and in 38.9 ± 7% of the cells Golgi stacks are fragmented, and vesicles are dispersed all over the cytosol (¶ in Figure 5A). In this case, the remaining Golgi measures 2.3 ± 0.7 μm in diameter.

To quantify the degree of dispersion, several parameters were measured: AOG (area occupied by Golgi); CF/A (cell fluorescence excluding the Golgi per unit of area), and GFL (% of fluorescence in the Golgi). As shown in Figure 5B, the area occupied by Golgi decreases in $A\beta^{25-35}$-treated cells, confirming that Aβ induces robust Golgi fragmentation in HeLa cells. When dispersion of the fragmented Golgi was measured, it showed that CF/A increases with $A\beta^{25-35}$ treatment, which was prevented by Cdk5 inhibition using either TAT-CIP or roscovitine. Finally, the percentage of fluorescence present in the Golgi decreased in $A\beta^{25-35}$-treated cells and increased in all samples where Cdk5 was inhibited, regardless of the presence of $A\beta^{25-35}$. The percentage of cells with fragmented Golgi was counted using an epifluorescence microscope, which correlated well with the result obtained using confocal microscope (Figure 5C). Dispersed vesicular immunostaining could be readily differentiated from juxtanuclear compact Golgi staining using an epifluorescence microscope, which confirmed that Aβ-induced Golgi fragmentation was prevented by Cdk5 inhibition (Figure 5C). Together, these results reveal a critical role of Cdk5 in causing Golgi fragmentation upon Aβ treatment (Figure 5, A–C).

Role of Cdk5 in Golgi Disassembly in PC12 Cells upon $A\beta^{25-35}$ and Glutamate Treatment

We next used differentiated neuronal cells as a model both to circumvent mitotic Golgi fragmentation and to study Cdk5 in a more physiological environment. PC12 were differentiated using NGF for 3 d, after which they were subjected to either Aβ (25 μM) or glutamate (10 mM) treatment for 24 h. Similar to Aβ, glutamate have also not been linked to Golgi fragmentation either. Both treatments induced robust Golgi fragmentation after 24 h, which was prevented only if TAT-CIP was present during this process (Figure 5, D and E). In contrast, roscovitine-mediated inhibition of Cdk5 during Aβ-treatment did not prevent Golgi disassembly, presumably because of its toxicity upon longer exposure (Figure 5, D and E).

Role of Cdk5 in Golgi Disassembly in SH-SY5Y Cells upon $A\beta^{25-35}$ and Glutamate Treatment

Human neuroblastoma SH-SY5Y cells undergo slow cell death upon exposure to both glutamate and Aβ and are used as a tissue culture model for AD. Therefore, these cells were selected next to investigate Cdk5's role in Golgi disassembly. Similar to PC12 cells, glutamate causes SH-SY5Y cell death due to oxytosis and increased Ca^{2+} levels (May *et al.*, 2006). SH-SY5Y cells were differentiated into neuronal like cells using retinoic acid for 5 d. Retinoic acid differentiation causes basal Golgi fragmentation (Sarkanen *et al.*, 2007). In this case, however, Golgi vesicles are not dispersed around the cell, but remain grouped next to the nucleus. Glutamate-treatment for 24 h resulted in strong Golgi disassembly (Figure 5, F and G). In this case, both TAT-CIP and roscovitine rescued Golgi disruption; however, roscovitine was not as efficient (Figure 5, F and G). When Aβ was used to induce Golgi fragmentation, it showed a similar pattern. These results strongly support Cdk5's role in Golgi fragmentation in AD downstream of Aβ and glutamate.

Role of Cdk5 in Golgi Disassembly in Primary Cortical Cells upon $A\beta^{25-35}$ and Glutamate Treatment

To investigate if Cdk5-mediated Golgi fragmentation is a common mechanism in primary neurons as well, primary cortical cells isolated from E-17 Sprague Dawley rats were subjected to Aβ and glutamate treatments. The percentage of cells with fragmented Golgi was monitored 24 h after Aβ stimulation and 12 h after glutamate treatment. Both Aβ and glutamate caused robust Golgi fragmentation, which was also Cdk5-dependent (Figure 6, A and B).

Sole Activation of Cdk5 Causes Golgi Fragmentation in Primary Cortical Cells

Because our result showed an essential role of Cdk5 in glutamate- and Aβ-induced Golgi fragmentation, we analyzed if Cdk5 hyperactivation was enough to induce fragmentation in the absence of other toxic stimuli. TAT-p25 transduction revealed strong Golgi fragmentation in 12 h (Figure 6, A and C), suggesting that Cdk5 activation alone is sufficient to induce fragmentation in the absence of other neurotoxic stimuli.

Sole Activation of Cdk5 Causes Golgi Fragmentation in PC12 and SH-SY5Y Cells

TAT-p25 was next transduced in differentiated PC12 and SH-SY5Y cells and Golgi disassembly analyzed at different times using anti-mannosidase immunostaining (Figure 6D). TAT-p25 treatment resulted in strong Golgi fragmentation, similar to the results obtained using primary neurons (Figure 6, C and E).

Aβ- and Glutamate-mediated Cell Death in Differentiated PC12 and SH-SY5Y is Cdk5-dependent

Both Aβ- and glutamate-induced toxicity in neurons have been shown to be largely Cdk5-dependent (Alvarez *et al.*, 1999; Lee *et al.*, 2000; Wei *et al.*, 2002; O'Hare *et al.*, 2005). As robust Golgi fragmentation was observed after 24 h of $A\beta^{25-35}$ and glutamate treatments in both differentiated PC12 and SH-SY5Y cells, we next investigated if these events lead to cell death.

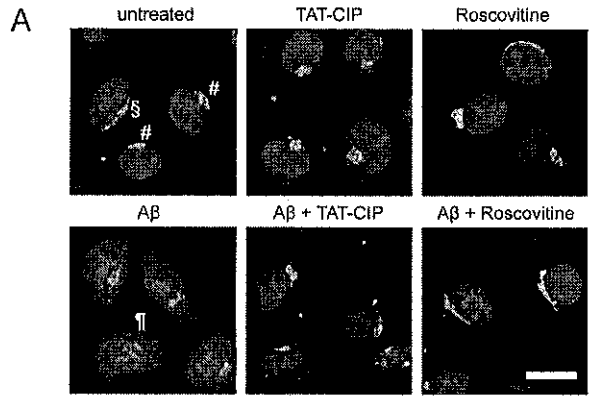

B

	AOG (μm^2)	CF/A (arbitrary units)	GFL (%)
control	22.7 ± 2.4	2.6 ± 0.2	13.2 ± 1.5
β-amyloid	10.4 ± 1.7 **	3.9 ± 0.2**	8.7 ± 0.8*
TAT-CIP	35.2 ± 11.2	2.2 ± 0.2	21.9 ± 3.8*
Roscovitine	29.4 ± 2.1	3.1 ± 0.2	19.1 ± 2.1*
TAT-CIP β-amyloid	27.2 ± 4.8	3.1 ± 0.1	20.4 ± 0.6*
Roscovitine β-amyloid	32.7 ± 2.2 *	2.5 ± 0.1	19.8 ± 2.1

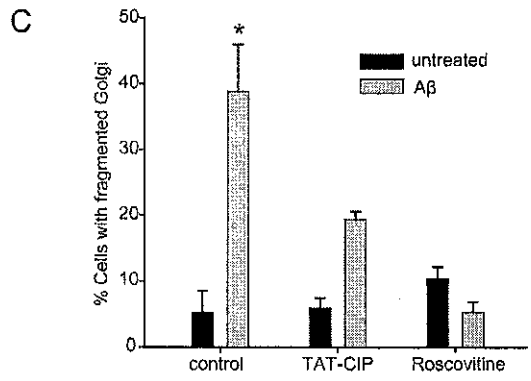

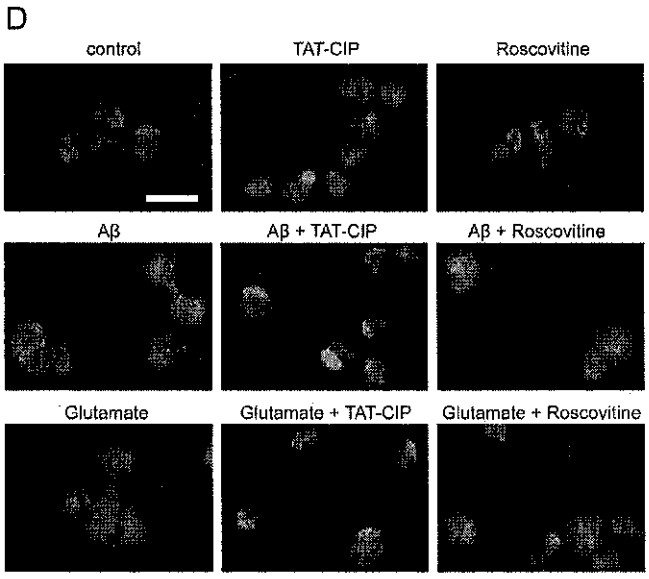

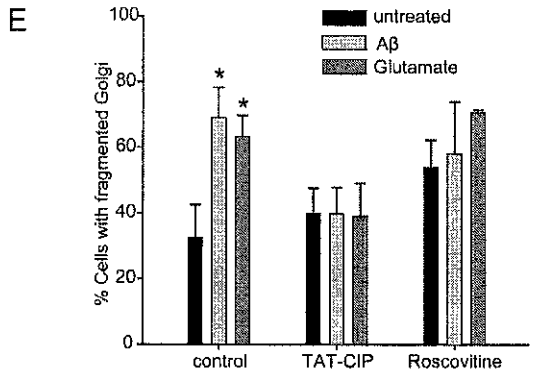

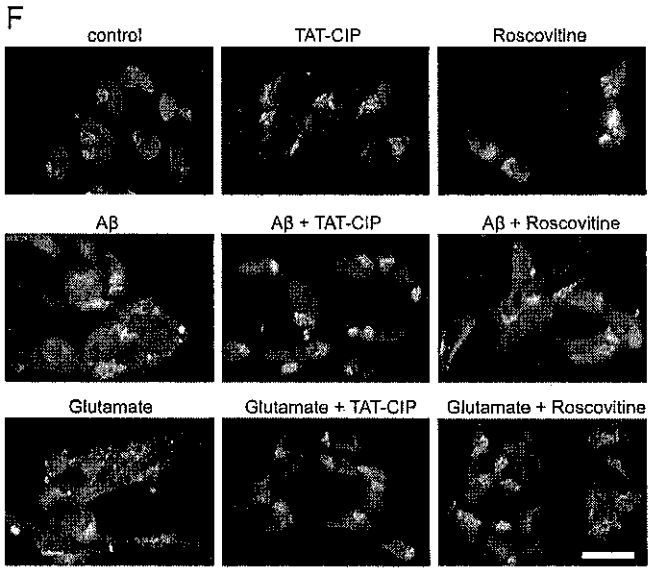

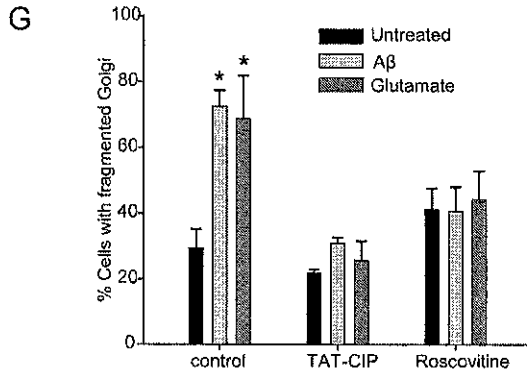

Figure 5. Cdk5 is involved in Golgi fragmentation induced by neurotoxic stimuli. (A) Serum-starved HeLa cells were treated with 200 nM TAT-CIP, 10 μM roscovitine, 100 μM $A\beta^{25-35}$, or the vehicle (no treatment) as indicated. After 12 h of treatment cells were fixed with methanol and immunostained with mannosidase II (green). DAPI was used to stain the nuclei (blue). Representative confocal pictures are shown. Scale bar, 20 μm. §, Golgi ribbon; #, round Golgi; and ¶, fragmented Golgi. (B) Morphological parameters quantification: confocal pictures from six cells for each condition were measured as described in *Materials and Methods*. AOG area of Golgi, CF/A mannosidase labeling intensity outside the Golgi, GFL percentage of fluorescence in the Golgi. *$p < 0.05$, **$p < 0.01$. (C) HeLa cells were treated and immunostained in the

Cell viability in differentiated PC12 and SH-SY5Y cells was quantified by MTT assay after 48–72 h of glutamate and Aβ treatments. For both treatments PC12 and SH-SY5Y cells showed significant loss in cell viability after 48 h. TAT-CIP treatment revealed it to be Cdk5-dependent both in SH-SY5Y and PC12 cells (Figure 7, A and B, respectively).

To further quantify cell death in glutamate and Aβ treated differentiated PC12 and SH-SY5Y cells, nuclear morphology was observed using propidium iodide. After neurotoxin treatments, cells were fixed and stained with PI at different time points and analyzed using fluorescence microscopy. Although few cells showed apoptotic nuclei after 24 h, they increased considerably after 48 h in both the cell types upon glutamate and Aβ treatment (Figure 7, D and F).

As shown in Figure 7, E and G (PC12 and SH-SY5Y, respectively), apoptotic nuclear counting revealed a similar trend: both glutamate and Aβ curtailed significant cell viability in 48 h, which was prevented if Cdk5 kinase activity was inhibited.

Golgi Fragmentation Alone Is Not Sufficient to Induce Cell Death

Because Golgi fragmentation may precede neuronal death (Nakagomi *et al.*, 2008), we next wanted to investigate if Cdk5-mediated Golgi fragmentation is enough to promote death. To this end, TAT-p25 was used to induce Golgi fragmentation. Robust Golgi fragmentation was observed at 12 h after TAT-p25 treatment in both differentiated PC12 and SH-SY5Y cells (Figure 6, D and E); however, cell death was only observed after 24 h (Figure 7, D, F, and H) but not at 12 h (data not shown). Similarly, Aβ and glutamate treatments in SH-SY5Y and PC12 cells also showed minimal cell death, but showed robust Golgi fragmentation at 24 h (Figure 7, A and B), suggesting that Golgi fragmentation may precede neuronal death, but is not enough to induce cell death. Because Golgi fragmentation has been suggested to be an early event in AD pathology (Baloyannis, 2006), it supports our hypothesis that Golgi fragmentation alone may not be sufficient to cause acute toxicity. Notably, TAT-p25, Aβ, and glutamate showed considerable toxicity in 48–72 h that was Cdk5-dependent (Figure 7, A–G). These findings suggest that Cdk5 activates other neurotoxic pathways as well causing toxicity (our unpublished data).

Mechanism of Cdk5-induced Golgi Fragmentation

To unravel the mechanism of Cdk5-mediated Golgi fragmentation, a chemical genetic screen was conducted to identify novel substrates of Cdk5 kinase in mouse brain lysates (Shah *et al.*, 1997; Shah and Shokat, 2002; Shah and Shokat, 2003; Shah and Vincent, 2005; Kim and Shah, 2007). Cdk5 was engineered to accept a nonnatural phosphate donor substrate (A*TP) that is poorly accepted by wild-type protein kinases in the cell (our unpublished observations). This analog-sensitive mutation was created in the active site of Cdk5 by replacing F80 with a glycine residue (Cdk5-analog–sensitive kinase-1, Cdk5-as1; our unpublished data). To identify the most optimal orthogonal phospho-donor for the engineered kinase, several [γ-^{32}P]ATP analogs were screened using Cdk5-as1/p25, which identified [γ-^{32}P]*N*-6-phenethyl-ATP as the optimal orthogonal phosphodonor for Cdk5-as1 kinase. This chemical genetic approach was used in conjunction with 2D electrophoresis and mass spectrometry to identify the direct substrates of Cdk5 in mouse brain extracts (our unpublished data).

This screen revealed *cis*-Golgi matrix protein GM130 as a novel substrate of Cdk5. Both Cdc2 and Cdk5 have similar substrate specificity and preferentially phosphorylate S/TP sites. As Cdc2 phosphorylates GM130 at Ser25, causing Golgi fragmentation, deregulated Cdk5 may also phosphorylate the same site resulting too in Golgi fragmentation. To examine this possibility, an in vitro kinase assay was conducted using Cdk5/p25 and GM130 immune complex isolated from HeLa cells. GM130 phosphorylation was probed using Ser25-phosphospecific GM130 antibody. Our result revealed that Cdk5 phosphorylates GM130 at Ser 25 (Figure 8A).

GM130 Phosphorylation Inhibits Its Binding to p115

GM130 phosphorylation at Ser25 should inhibit its binding to vesicle-docking protein p115 causing Golgi disassembly (Nakamura *et al.*, 1997). To investigate this possibility, 6-His–tagged GM130 was expressed, purified, and subjected to kinase assay with Cdk5/p25. p115 was expressed in HeLa cells using transfection and isolated using FLAG antibody. Untreated and Cdk5/p25-treated GM130 were added to p115 beads, and their binding was investigated. GM130 phosphorylation abrogates its binding to p115 (Figure 8B).

Aβ Treatment Causes GM130 Phosphorylation and Inhibits p115 Binding

To confirm the relevance of Cdk5-mediated GM130 phosphorylation in a cellular context, HeLa cells were transfected with GM130, serum-starved, and treated with Aβ to induce Golgi fragmentation. GM130 was phosphorylated at Ser25 upon Aβ treatment, which was prevented upon Cdk5 inhibition (Figure 8C, top panel). These results were further confirmed by investigating p115 binding, which decreased substantially upon GM130 phosphorylation, which was Cdk5-dependent as expected (Figure 8C, middle panel).

Sole Activation of Cdk5 Promotes GM130 Phosphorylation and Inhibits p115 Binding

Next, TAT-p25 was transduced in HeLa cells and GM130 phosphorylation was investigated. GM130 phosphorylation at Ser25 increased substantially in 3 h with simultaneous dissociation of p115 (Figure 8D). Together, these results suggest that GM130 phosphorylation by Cdk5 is an important mechanism by which Golgi fragmentation can occur in AD. As deregulated Cdk5 activity is reported in several neurodegenerative diseases that show Golgi fragmentation as well, the phenomenon may be Cdk5-dependent.

Figure 5 (cont). same way as in A. Percentage of cells with fragmented Golgi was scored as percentage of cells with significant cytosolic labeling and small remaining Golgi using an epifluorescence microscope; 100 cells were counted for each sample in triplicates. *$p < 0.05$. (D) Differentiated PC12 were treated with 25 μM $A\beta^{25-35}$ or 10 mM glutamate for 24 h in the presence of 200 nM TAT-CIP, 10 μM roscovitine or the vehicle as described in *Materials and Methods*. Representative pictures from methanol fixed cells stained with anti-mannosidase II (red) and DAPI (blue) are shown. Scale bar, 20 μm. (E) Graph shows the percentage of differentiated PC12 cells with fragmented Golgi, i.e., diffused Golgi staining in the cytosol. Average of 100 cells from five random fields; *$p < 0.05$. (F) Differentiated SH-SY5Y were treated with 25 μM $A\beta^{25-35}$ or 10 mM glutamate for 24 h in the presence of 200 nM TAT-CIP, 10 μM roscovitine, or the vehicle as described in *Materials and Methods*. Representative pictures from methanol-fixed cells stained with anti-mannosidase II (green) and DAPI (blue) are shown. Scale bar, 20 μm. (G) Quantification: percentage of SH-SY5Y cells with diffused Golgi staining in the cytosol. Average of 100 cells from five random fields; *$p < 0.05$.

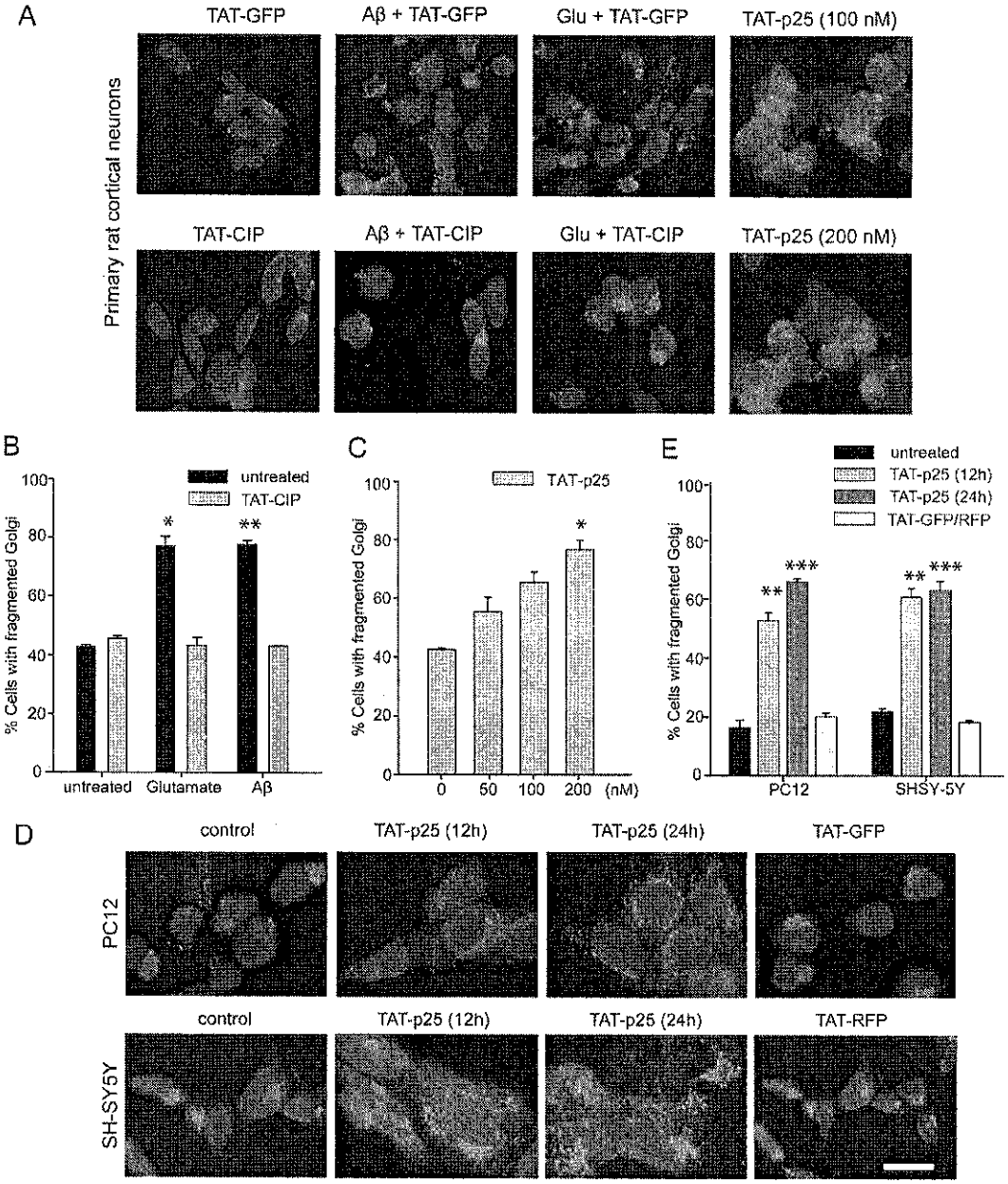

Figure 6. (A) Rat cortical cells plated on coverslips were used on DIV5. TAT-CIP or TAT-GFP at 200 nM were added 30 min before adding glutamate or $A\beta^{25-35}$. Cells were treated with 10 mM glutamate, 25 μM $A\beta^{25-35}$, or different amounts of TAT-p25. All recombinant TAT proteins were readded every 4 h. After 12 h (glutamate and TAT-p25) or 24 h ($A\beta^{25-35}$ treatment) cells were fixed and immunostained using mannosidase II antibody to detect Golgi (red) and Hoechst was used to stain the nuclei (blue). Percentage of cells with fragmented Golgi were counted from a total 300 cells from random fields in duplicates (B and C). (D) TAT-p25 induces Golgi fragmentation. Differentiated PC12 and SH-SH5Y cells were transduced with 200 nM TAT-p25, 200 nM TAT-GFP (PC12), or TAT-RFP (SH-SY5Y); 0.5 mM imidazole was used as a control. After 12 and 24 h of sustained addition of protein, cells were fixed and immunostained against mannosidase II with a second antibody red (PC12) or green (SH-SY5Y), together with DAPI (blue). Scale bar, 20 μm. (E) Quantification of the percentage of cells with fragmented Golgi. Average of 100 cells counted from five different random fields; $^*p < 0.05$, $^{**}p < 0.01$, $^{***}p < 0.001$.

DISCUSSION

Golgi apparatus plays a central role in posttranslational modification, transport, and targeting of a variety of proteins destined for lysosomes, plasma membrane, or secretion. Newly synthesized proteins in neurons are processed through Golgi for fast axoplasmic transport. Fragmentation of Golgi apparatus during mitosis is a physiological phenomenon, during which Golgi is disassembled in early prophase and later reassembled in telophase (Robbins and Gonatas, 1964). Pathologically, neuronal Golgi apparatus is fragmented or dispersed in a variety of neurodegenerative diseases. A recent study has shown that expression of C-terminal fragment of Golgi-associated protein GRASP65 (G65Δ200) prevents mitotic Golgi disassembly (Sutterlin *et al.*, 2002), but only partially rescues Golgi fragmentation initiated via apoptotic

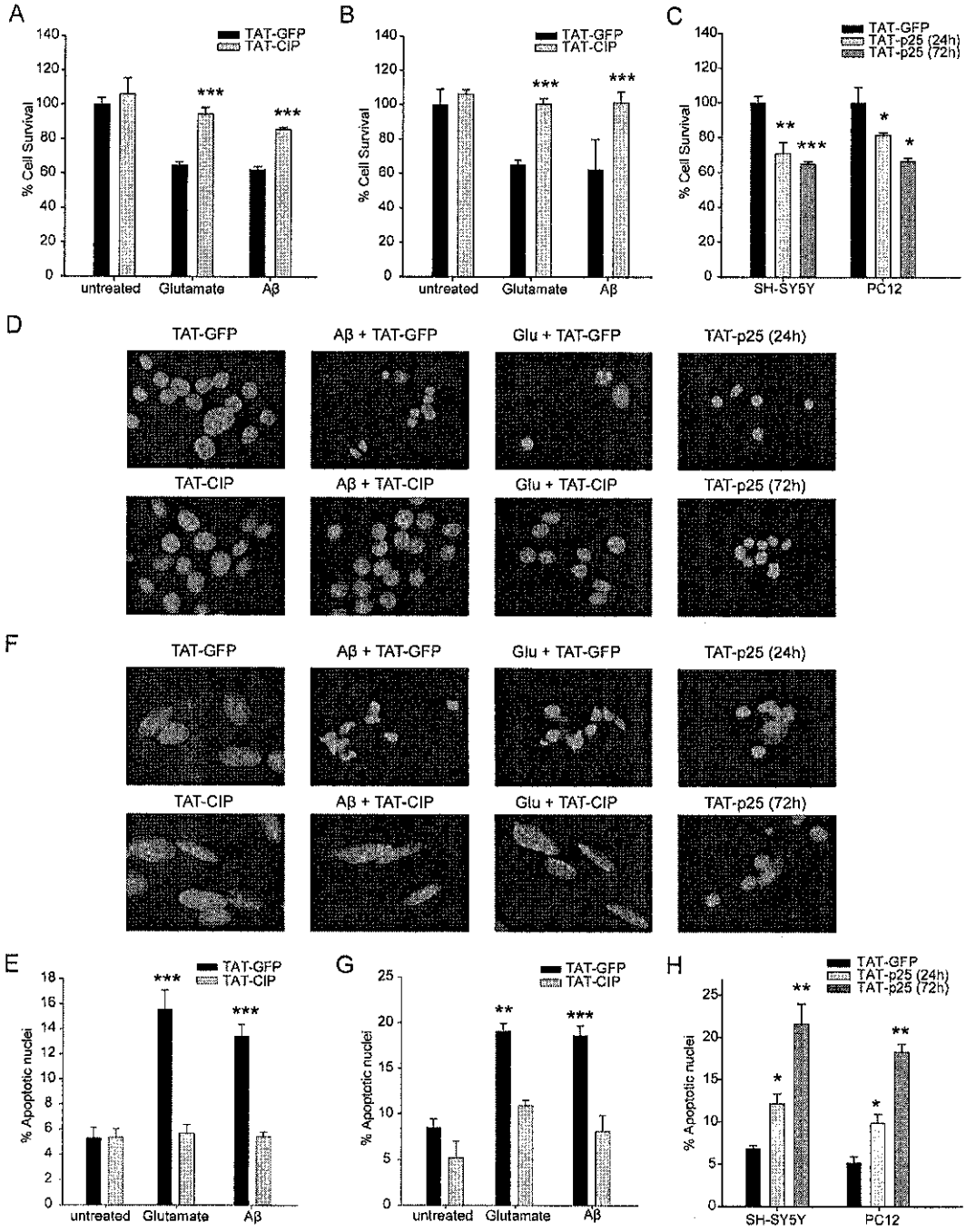

Figure 7. Differentiated SH-SY5Y (A) and PC12 (B) cells were treated with 10 mM glutamate for up to 48 h or 25 μM Aβ^{25-35} for 72 h in the presence of 200 nM TAT-CIP or TAT-GFP (C) or with 200 nM TAT-p25 for 24 and 72 h. All recombinant proteins were added every 4 h. Cell viability was measured at the end of the treatment by the addition of MTT reagent for 30 min, and cells were rinsed with PBS and lysed in DMSO. Graph presents the percentage of absorbance (in proportion to cell viability) compared with the TAT-GFP–treated control. Differentiated PC12 (D) or SH-SY5Y (F) were treated with 10 mM glutamate or 25 μM Aβ^{25-35} in the presence of 200 nM TAT-CIP or TAT-GFP for 48 h or with 200 nM TAT-p25 for up to 24 or 72 h. All recombinant proteins were added every 4 h. After treatment, cells were fixed and permeabilized, and nuclei were stained with PI (red). The percentage of cells with apoptotic nuclei (pycnotic or fragmented) is shown (E, G, and H); 300 cells from random fields were counted in duplicate. *$p < 0.05$, **$p < 0.01$, ***$p < 0.001$.

insult (Nakagomi *et al.*, 2008). These findings suggest that irreversible Golgi dispersion in degenerating brains may be catalyzed by additional neurotoxic signals. Because aberrant Cdk5 activity is present in several neurodegenerative disorders, the goal of the present study was to investigate if a relationship exists between deregulated Cdk5 activity and Golgi fragmentation in AD.

Two popular methods have been used to probe Cdk5's role, constitutive expression of Cdk5 activators and inhibition using small molecule inhibitors (e.g., roscovitine). Stud-

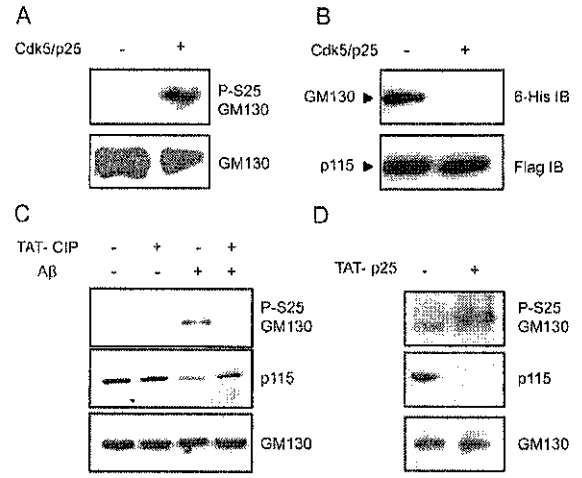

Figure 8. (A) GM130 is phosphorylated by Cdk5. GM130 immunoprecipitated from HeLa cells was used as a substrate for Cdk5/p25 (right lane) or loaded directly (left lane) and probed in a Western blot with phospho-serine 25-GM130–specific antibody (top panel) and stripped and reprobed with total GM130 as a loading control (bottom panel). (B) Soluble recombinant 6-His-GM130 was phosphorylated in vitro with Cdk5/p25 (+) or used directly (−). Flag-p115 was immunoprecipitated from HeLa cells and used for binding with GM130. Bound proteins were resolved in SDS-PAGE and 6-His-GM130 was detected by Western blot (top panel). The same samples were blotted in parallel against FLAG-p115 to check the IP efficiency (bottom panel). (C) HeLa cells were transfected with myc-GM130. Serum starvation was initiated 12 h after transfection and was continued for 24 h. TAT-CIP was added as indicated 30 min before 100 μM β-amyloid treatment. After 12 h, GM130 was immunoprecipitated, and GM130 phosphorylation and p115 binding were detected by Western blot (top and middle panel). Total GM130 is shown in the bottom panel as loading control. (D) GM130-transfected HeLa cells were serum-starved for 20 h and transduced with TAT-p25 for 3 h. GM130 Ser25 phosphorylation is shown in the top panel. P115 bound to immunoprecipitated GM130 was detected by Western blot (middle panel), and total GM130 was used as loading control.

ies in p25 transgenic mice that compared chronic and inducible activation of Cdk5 led to different pathological consequences (Takashima *et al.*, 2001; Cruz *et al.*, 2003). Constitutive activation did not result in tau hyperphosphorylation or neuronal damage (Takashima *et al.*, 2001). Inducible activation, on the other hand, caused NFT formation, astrogliosis and extensive neurodegeneration (Cruz *et al.*, 2003). Thus, Cdk5 deregulation may have fatal consequences in the cell, but its activity can be masked by a compensatory mechanism if expressed constitutively.

Chemical inhibitors of Cdk5 provide high temporal control, but are not absolutely specific. Roscovitine, the most widely used molecule, is also a potent inhibitor of Cdc2 and Cdk2 (Meijer *et al.*, 1997). It also inhibits Cdk5, Cdc2/cyclin B, Cdk2/cyclin A, and Cdk2/cyclin E with an IC50 of 200, 650, 700, and 700 nM, respectively. As roscovitine is commonly used at 10–100 μM concentrations, it may inhibit other Cdks significantly (especially Cdc2), leading to cell cycle arrest or cell death. This could be particularly disadvantageous for dissecting Cdk5's role in cell survival and cell death pathways, as Cdk5 can be proapoptotic or antiapoptotic.

Recent studies have utilized small interference RNA (siRNA) of Cdk5 to eliminate its activity (Griffin *et al.*, 2004; Lin *et al.*, 2004; Song *et al.*, 2005; Kanungo *et al.*, 2006, 2007; Strock *et al.*, 2006; Li *et al.*, 2007; Zheng *et al.*, 2007). Although faster than the traditional gene knockout approach, siRNA modulates Cdk5 levels slowly (~24–48 h) and lacks dosage control. In addition, the sequence specificity for Cdk5 siRNA varies in different species and cell types and needs to be optimized for each cell type.

Because none of the available methods were suitable for deconvoluting Cdk5's role in Golgi disassembly, we developed highly specific and temporal modulators of Cdk5. The key feature of our approach is to fuse modulators specific for Cdk5 with the TAT sequence to create transducible proteins. TAT-fusion protein can enter primary cells, alleviating the need for transfection, which is relatively inefficient. Although lentiviral infection is efficient for primary cells, it lacks temporal control. TAT-fusion protein should allow for a rapid readout in primary neurons with very high efficiency.

TAT-p25 proved to be a potent inducible tool for specific and temporal activation of Cdk5 in various cells, including primary neurons. The temporal control afforded by this approach prevents any cellular compensation. By tightly controlling Cdk5 activation levels using TAT-p25, additional Cdk5 substrates and their functions may be uncovered.

On the other hand, TAT-CIP is an inhibitor specific for Cdk5 with high temporal control. TAT-CIP inhibits Cdk5 in vitro (Amin *et al.*, 2002; Figure 2, B and D) and in cells downstream of various stimuli (glutamate and $A\beta^{25-35}$; Figure 3, A–C), when added before Cdk5/p25 complex formation. Although CIP does not inhibit Cdk5/p35 when expressed endogenously (Zheng *et al.*, 2002, 2005), our data show that TAT-CIP inhibits Cdk5/p35 if added before complex formation in vitro (Figure 2, B and D). NGF-induced neuronal differentiation in PC12 cells depends on p35 upregulation and consequently p35-mediated Cdk5 activation. Thus, inhibition of neurite outgrowth by TAT-CIP supports the same conclusion in the cells (Figure 4, A and B).

We next proceeded to evaluate Cdk5's role in Golgi fragmentation. Robust fragmentation was observed upon Aβ and glutamate stimulation in differentiated PC12 and SH-SY5Y cells and primary neurons. Golgi disassembly was fully rescued if Cdk5 was inhibited using TAT-CIP, suggesting Cdk5's vital role in Golgi disassembly. Inhibition with roscovitine, in contrast, did not prevent Golgi fragmentation as well, presumably due to its toxic side effects as noted above. Cdk5's role was further confirmed using TAT-p25, which caused robust Golgi fragmentation without any other input.

To delineate the mechanism leading to Golgi fragmentation via Cdk5, we identified GM130 as a novel substrate of Cdk5 using a chemical genetic screen. GM130 is phosphorylated by Cdc2 at the onset of early prophase and remains so during metaphase and anaphase (Lowe *et al.*, 1998). Phosphorylation occurs at serine-25, disrupting the interaction between GM130 and vesicle-docking protein p115, causing Golgi fragmentation. GM130 is dephosphorylated during telophase, resulting in Golgi reassembly (Lowe *et al.*, 1998). As Cdc2 and Cdk5 have similar substrate specificity, it suggested that Cdk5 may act in a similar manner as Cdc2. Cdk5 indeed phosphorylates this SP site upon Aβ stimulation, which inhibits it's binding to p115, suggesting that Cdk5 may cause Golgi fragmentation upon deregulation via a similar mechanism. Notably, our results further show that Golgi fragmentation alone is not sufficient trigger for acute toxicity.

In conclusion, TAT-p25 and TAT-CIP were developed, which specifically activate and inhibit Cdk5 activity, respec-

tively, in vitro and in the cells. With the help of these tools, we show a critical role for Cdk5 in Golgi fragmentation in AD. In contrast, roscovitine was relatively toxic presumably due to Cdc2 and Cdk2 inhibition, especially upon prolonged incubation (>24 h). This finding reinforces the importance of the novel tools developed in this study. Although, an earlier study identified a physiological function for Cdk5/p35 in Golgi apparatus in regulating membrane traffic during neuronal process outgrowth (Paglini *et al.*, 2001), this is the first report that shows a pathological role of Cdk5 in disrupting Golgi apparatus.

Inducible control over Cdk5 activity using either transient or sustained addition of Cdk5 modulators should provide useful tools to dissect Cdk5's function in various cell types. Moreover, because TAT-CIP is highly specific for Cdk5, it may be especially useful for isolating Cdk5's role downstream of different biological stimuli. Due to the high specificity of the TAT-fusion Cdk5 modulators, these genetic approaches should be valuable additions to researchers' toolkits for the functional study of Cdk5 in various cellular processes. As all Cdks require cyclin binding partners, these approaches can be extended to other family members too. Finally, as Golgi disassembly is a common occurrence in many neurodegenerative diseases, this study suggests a vital role for Cdk5 in other diseases as well.

ACKNOWLEDGMENTS

We thank Laurent Meijer (CNRS, France) for GST-Cdk5, Steve Dowdy (University of California, San Diego) for pET-28b-TAT (V2.1) and pTAT-HA vectors, Roger Tsein for mPlum-RFP, David Schubert (Salk Institute) for HT22 cells, Dennis Shields (Albert Einstein College of Medicine of Yeshiva University) for p115 cDNA and antibody, and Martin Lowe (University of Manchester, United Kingdom) for phosphospecific GM130 antibody. This work was supported by Purdue Research Foundation and Walther Cancer Institute.

REFERENCES

Acharya, U., Mallabiabarrena, A., Acharya, J. K., and Malhotra, V. (1998). Signaling via mitogen-activated protein kinase kinase (MEK1) is required for Golgi fragmentation during mitosis. Cell *92*, 183–192.

Altan-Bonnet, N., Sougrat, R., and Lippincott-Schwartz, J. (2004). Molecular basis for Golgi maintenance and biogenesis. Curr. Opin. Cell Biol. *16*, 364–372.

Alvarez, A., Toro, R., Caceres, A., and Maccioni, R. B. (1999). Inhibition of tau phosphorylating protein kinase cdk5 prevents beta-amyloid-induced neuronal death. FEBS Lett. *459*, 421–426.

Amin, N. D., Albers, W., and Pant, H. C. (2002). Cyclin-dependent kinase 5 (cdk5) activation requires interaction with three domains of p35. J. Neurosci. Res. *67*, 354–362.

Augustinack, J. C., Sanders, J. L., Tsai, L. H., and Hyman, B. T. (2002). Colocalization and fluorescence resonance energy transfer between cdk5 and AT8 suggests a close association in pre-neurofibrillary tangles and neurofibrillary tangles. J. Neuropathol. Exp. Neurol. *61*, 557–564.

Baloyannis, S. J. (2006). Mitochondrial alterations in Alzheimer's disease. J. Alzheimers Dis. *9*, 119–126.

Beaudette, K. N., Lew, J., and Wang, J. H. (1993). Substrate specificity characterization of a cdc2-like protein kinase purified from bovine brain. J. Biol. Chem. *268*, 20825–20830.

Becker-Hapak, M., McAllister, S. S., and Dowdy, S. F. (2001). TAT-mediated protein transduction into mammalian cells. Methods *24*, 247–256.

Becker-Hapak, M., and Dowdy, S. F. (2003). Protein transduction: generation of full-length transducible proteins using the TAT system. Curr. Protoc. Cell Biol. Chapter *20*, Unit 20.2.

Benavides, D. R., and Bibb, J. A. (2004). Role of Cdk5 in drug abuse and plasticity. Ann. NY Acad. Sci. *1025*, 335–344.

Billings, L. M., Oddo, S., Green, K. N., McGaugh, J. L., and LaFerla, F. M. (2005). Intraneuronal Abeta causes the onset of early Alzheimer's disease-related cognitive deficits in transgenic mice. Neuron *45*, 675–688.

Casas, C. *et al.* (2004). Massive CA1/2 neuronal loss with intraneuronal and N-terminal truncated Abeta42 accumulation in a novel Alzheimer transgenic model. Am. J. Pathol. *165*, 1289–1300.

Colanzi, A., and Corda, D. (2007). Mitosis controls the Golgi and the Golgi controls mitosis. Curr. Opin. Cell Biol. *19*, 386–393.

Colanzi, A., Suetterlin, C., and Malhotra, V. (2003). Cell-cycle-specific Golgi fragmentation: how and why? Curr. Opin. Cell Biol. *15*, 462–467.

Cruz, J. C., Kim, D., Moy, L. Y., Dobbin, M. M., Sun, X., Bronson, R. T., and Tsai, L. H. (2006). p25/cyclin-dependent kinase 5 induces production and intraneuronal accumulation of amyloid beta in vivo. J. Neurosci. *26*, 10536–10541.

Cruz, J. C., and Tsai, L. H. (2004). Cdk5 deregulation in the pathogenesis of Alzheimer's disease. Trends Mol. Med. *10*, 452–458.

Cruz, J. C., Tseng, H. C., Goldman, J. A., Shih, H., and Tsai, L. H. (2003). Aberrant Cdk5 activation by p25 triggers pathological events leading to neurodegeneration and neurofibrillary tangles. Neuron *40*, 471–483.

Chae, T., Kwon, Y. T., Bronson, R., Dikkes, P., Li, E., and Tsai, L. H. (1997). Mice lacking p35, a neuronal specific activator of Cdk5, display cortical lamination defects, seizures, and adult lethality. Neuron *18*, 29–42.

Chang, T. S., Jeong, W., Choi, S. Y., Yu, S., Kang, S. W., and Rhee, S. G. (2002). Regulation of peroxiredoxin I activity by Cdc2-mediated phosphorylation. J. Biol. Chem. *277*, 25370–25376.

Cheng, G., Whitehead, S. N., Hachinski, V., and Cechetto, D. F. (2006). Effects of pyrrolidine dithiocarbamate on beta-amyloid (25–35)-induced inflammatory responses and memory deficits in the rat. Neurobiol. Dis. *23*, 140–151.

Chiu, R., Novikov, L., Mukherjee, S., and Shields, D. (2002). A caspase cleavage fragment of p115 induces fragmentation of the Golgi apparatus and apoptosis. J. Cell Biol. *159*, 637–648.

Dhavan, R., and Tsai, L. H. (2001). A decade of CDK5. Nat. Rev. Mol. Cell Biol. *2*, 749–759.

Dzubay, J. A., and Jahr, C. E. (1999). The concentration of synaptically released glutamate outside of the climbing fiber-Purkinje cell synaptic cleft. J. Neurosci. *19*, 5265–5274.

Fischer, A., Sananbenesi, F., Pang, P. T., Lu, B., and Tsai, L. H. (2005). Opposing roles of transient and prolonged expression of p25 in synaptic plasticity and hippocampus-dependent memory. Neuron *48*, 825–838.

Fischer, A., Sananbenesi, F., Spiess, J., and Radulovic, J. (2003). Cdk5 in the adult non-demented brain. Curr. Drug Targets CNS Neurol. Disord. *2*, 375–381.

Gonatas, N. K., Stieber, A., and Gonatas, J. O. (2006). Fragmentation of the Golgi apparatus in neurodegenerative diseases and cell death. J. Neurol. Sci. *246*, 21–30.

Gong, X., Tang, X., Wiedmann, M., Wang, X., Peng, J., Zheng, D., Blair, L. A., Marshall, J., and Mao, Z. (2003). Cdk5-mediated inhibition of the protective effects of transcription factor MEF2 in neurotoxicity-induced apoptosis. Neuron *38*, 33–46.

Goodyear, S., and Sharma, M. C. (2007). Roscovitine regulates invasive breast cancer cell (MDA-MB231) proliferation and survival through cell cycle regulatory protein cdk5. Exp. Mol. Pathol. *82*, 25–32.

Gouras, G. K. *et al.* (2000). Intraneuronal Abeta42 accumulation in human brain. Am. J. Pathol. *156*, 15–20.

Gray, N., Detivaud, L., Doerig, C., and Meijer, L. (1999). ATP-site directed inhibitors of cyclin-dependent kinases. Curr. Med. Chem. *6*, 859–875.

Greene, L. A., and Tischler, A. S. (1976). Establishment of a noradrenergic clonal line of rat adrenal pheochromocytoma cells which respond to nerve growth factor. Proc. Natl. Acad. Sci. USA *73*, 2424–2428.

Griffin, S. V., Hiromura, K., Pippin, J., Petermann, A. T., Blonski, M. J., Krofft, R., Takahashi, S., Kulkarni, A. B., and Shankland, S. J. (2004). Cyclin-dependent kinase 5 is a regulator of podocyte differentiation, proliferation, and morphology. Am. J. Pathol. *165*, 1175–1185.

Harada, T., Morooka, T., Ogawa, S., and Nishida, E. (2001). ERK induces p35, a neuron-specific activator of Cdk5, through induction of Egr1. Nat. Cell Biol. *3*, 453–459.

Jang, H. H. *et al.* (2006). Phosphorylation and concomitant structural changes in human 2-Cys peroxiredoxin isotype I differentially regulate its peroxidase and molecular chaperone functions. FEBS Lett. *580*, 351–355.

Kang, S. W., Rhee, S. G., Chang, T. S., Jeong, W., and Choi, M. H. (2005). 2-Cys peroxiredoxin function in intracellular signal transduction: therapeutic implications. Trends Mol. Med. *11*, 571–578.

Kanungo, J., Li, B. S., Goswami, M., Zheng, Y. L., Ramchandran, R., and Pant, H. C. (2007). Cloning and characterization of zebrafish (*Danio rerio*) cyclin-dependent kinase 5. Neurosci. Lett. *412*, 233–238.

Kanungo, J., Li, B. S., Zheng, Y., and Pant, H. C. (2006). Cyclin-dependent kinase 5 influences Rohon-Beard neuron survival in zebrafish. J. Neurochem. *99*, 251–259.

Kim, S., and Shah, K. (2007). Dissecting yeast Hog1 MAP kinase pathway using a chemical genetic approach. FEBS Lett. *581*, 1209–1216.

Kitazawa, M., Oddo, S., Yamasaki, T. R., Green, K. N., and LaFerla, F. M. (2005). Lipopolysaccharide-induced inflammation exacerbates tau pathology by a cyclin-dependent kinase 5-mediated pathway in a transgenic model of Alzheimer's disease. J. Neurosci. *25*, 8843–8853.

Klementiev, B., Novikova, T., Novitskaya, V., Walmod, P. S., Dmytriyeva, O., Pakkenberg, B., Berezin, V., and Bock, E. (2007). A neural cell adhesion molecule-derived peptide reduces neuropathological signs and cognitive impairment induced by Abeta25-35. Neuroscience *145*, 209–224.

Ko, J., Humbert, S., Bronson, R. T., Takahashi, S., Kulkarni, A. B., Li, E., and Tsai, L. H. (2001). p35 and p39 are essential for cyclin-dependent kinase 5 function during neurodevelopment. J. Neurosci. *21*, 6758–6771.

Kubo, T., Nishimura, S., Kumagae, Y., and Kaneko, I. (2002). In vivo conversion of racemized beta-amyloid ([D-Ser 26]A beta 1–40) to truncated and toxic fragments ([D-Ser 26]A beta 25–35/40) and fragment presence in the brains of Alzheimer's patients. J. Neurosci. Res. *70*, 474–483.

Lane, J. D., Lucocq, J., Pryde, J., Barr, F. A., Woodman, P. G., Allan, V. J., and Lowe, M. (2002). Caspase-mediated cleavage of the stacking protein GRASP65 is required for Golgi fragmentation during apoptosis. J. Cell Biol. *156*, 495–509.

Lau, L. F., and Ahlijanian, M. K. (2003). Role of cdk5 in the pathogenesis of Alzheimer's disease. Neurosignals *12*, 209–214.

Lee, K. Y., Rosales, J. L., Tang, D., and Wang, J. H. (1996). Interaction of cyclin-dependent kinase 5 (Cdk5) and neuronal Cdk5 activator in bovine brain. J. Biol. Chem. *271*, 1538–1543.

Lee, M. S., Kwon, Y. T., Li, M., Peng, J., Friedlander, R. M., and Tsai, L. H. (2000). Neurotoxicity induces cleavage of p35 to p25 by calpain. Nature *405*, 360–364.

Lew, J., Huang, Q. Q., Qi, Z., Winkfein, R. J., Aebersold, R., Hunt, T., and Wang, J. H. (1994). A brain-specific activator of cyclin-dependent kinase 5. Nature *371*, 423–426.

Li, T., Chalifour, L. E., and Paudel, H. K. (2007). Phosphorylation of protein phosphatase 1 by cyclin-dependent protein kinase 5 during nerve growth factor-induced PC12 cell differentiation. J. Biol. Chem. *282*, 6619–6628.

Lin, H., Chen, M. C., Chiu, C. Y., Song, Y. M., and Lin, S. Y. (2007). Cdk5 regulates STAT3 activation and cell proliferation in medullary thyroid carcinoma cells. J. Biol. Chem. *282*, 2776–2784.

Lin, H., Juang, J. L., and Wang, P. S. (2004). Involvement of Cdk5/p25 in digoxin-triggered prostate cancer cell apoptosis. J. Biol. Chem. *279*, 29302–29307.

Liu, W. K., Williams, R. T., Hall, F. L., Dickson, D. W., and Yen, S. H. (1995). Detection of a Cdc2-related kinase associated with Alzheimer paired helical filaments. Am. J. Pathol. *146*, 228–238.

Lowe, M., Lane, J. D., Woodman, P. G., and Allan, V. J. (2004). Caspase-mediated cleavage of syntaxin 5 and giantin accompanies inhibition of secretory traffic during apoptosis. J. Cell Sci. *117*, 1139–1150.

Lowe, M., Rabouille, C., Nakamura, N., Watson, R., Jackman, M., Jamsa, E., Rahman, D., Pappin, D. J., and Warren, G. (1998). Cdc2 kinase directly phosphorylates the cis-Golgi matrix protein GM130 and is required for Golgi fragmentation in mitosis. Cell *94*, 783–793.

Mancini, M., Machamer, C. E., Roy, S., Nicholson, D. W., Thornberry, N. A., Casciola-Rosen, L. A., and Rosen, A. (2000). Caspase-2 is localized at the Golgi complex and cleaves golgin-160 during apoptosis. J. Cell Biol. *149*, 603–612.

Mapelli, M., Massimiliano, L., Crovace, C., Seeliger, M. A., Tsai, L. H., Meijer, L., and Musacchio, A. (2005). Mechanism of CDK5/p25 binding by CDK inhibitors. J. Med. Chem. *48*, 671–679.

Marshall, C. J. (1995). Specificity of receptor tyrosine kinase signaling: transient versus sustained extracellular signal-regulated kinase activation. Cell *80*, 179–185.

Maurice, T., Su, T. P., and Privat, A. (1998). Sigma1 (sigma 1) receptor agonists and neurosteroids attenuate B25-35-amyloid peptide-induced amnesia in mice through a common mechanism. Neuroscience *83*, 413–428.

May, J. M., Li, L., Hayslett, K., and Qu, Z. C. (2006). Ascorbate transport and recycling by SH-SY5Y neuroblastoma cells: response to glutamate toxicity. Neurochem. Res. *31*, 785–794.

Meijer, L., Borgne, A., Mulner, O., Chong, J. P., Blow, J. J., Inagaki, N., Inagaki, M., Delcros, J. G., and Moulinoux, J. P. (1997). Biochemical and cellular effects of roscovitine, a potent and selective inhibitor of the cyclin-dependent kinases cdc2, cdk2 and cdk5. Eur. J. Biochem. *243*, 527–536.

Monaco, E. A., 3rd. (2004). Recent evidence regarding a role for Cdk5 dysregulation in Alzheimer's disease. Curr. Alzheimer Res. *1*, 33–38.

Mukherjee, S., Chiu, R., Leung, S. M., and Shields, D. (2007). Fragmentation of the Golgi apparatus: an early apoptotic event independent of the cytoskeleton. Traffic *8*, 369–378.

Nagahara, H., Vocero-Akbani, A. M., Snyder, E. L., Ho, A., Latham, D. G., Lissy, N. A., Becker-Hapak, M., Ezhevsky, S. A., and Dowdy, S. F. (1998). Transduction of full-length TAT fusion proteins into mammalian cells: TAT-p27Kip1 induces cell migration. Nat. Med. *4*, 1449–1452.

Nakagomi, S., Barsoum, M. J., Bossy-Wetzel, E., Sutterlin, C., Malhotra, V., and Lipton, S. A. (2008). A Golgi fragmentation pathway in neurodegeneration. Neurobiol. Dis. *29*, 221–231.

Nakamura, N., Lowe, M., Levine, T. P., Rabouille, C., and Warren, G. (1997). The vesicle docking protein p115 binds GM130, a cis-Golgi matrix protein, in a mitotically regulated manner. Cell *89*, 445–455.

Nikolic, M., Dudek, H., Kwon, Y. T., Ramos, Y. F., and Tsai, L. H. (1996). The cdk5/p35 kinase is essential for neurite outgrowth during neuronal differentiation. Genes Dev. *10*, 816–825.

Noble, W. *et al.* (2003). Cdk5 is a key factor in tau aggregation and tangle formation in vivo. Neuron *38*, 555–565.

O'Hare, M. J., Kushwaha, N., Zhang, Y., Aleyasin, H., Callaghan, S. M., Slack, R. S., Albert, P. R., Vincent, I., and Park, D. S. (2005). Differential roles of nuclear and cytoplasmic cyclin-dependent kinase 5 in apoptotic and excitotoxic neuronal death. J. Neurosci. *25*, 8954–8966.

Oddo, S., Caccamo, A., Shepherd, J. D., Murphy, M. P., Golde, T. E., Kayed, R., Metherate, R., Mattson, M. P., Akbari, Y., and LaFerla, F. M. (2003). Triple-transgenic model of Alzheimer's disease with plaques and tangles: intracellular Abeta and synaptic dysfunction. Neuron *39*, 409–421.

Ohshima, T., Ward, J. M., Huh, C. G., Longenecker, G., Veeranna, Pant, H. C., Brady, R. O., Martin, L. J., and Kulkarni, A. B. (1996). Targeted disruption of the cyclin-dependent kinase 5 gene results in abnormal corticogenesis, neuronal pathology and perinatal death. Proc. Natl. Acad. Sci. USA *93*, 11173–11178.

Paglini, G., Peris, L., Diez-Guerra, J., Quiroga, S., and Caceres, A. (2001). The Cdk5–p35 kinase associates with the Golgi apparatus and regulates membrane traffic. EMBO Rep. *2*, 1139–1144.

Paglini, G., Pigino, G., Kunda, P., Morfini, G., Maccioni, R., Quiroga, S., Ferreira, A., and Caceres, A. (1998). Evidence for the participation of the neuron-specific CDK5 activator P35 during laminin-enhanced axonal growth. J. Neurosci. *18*, 9858–9869.

Patrick, G. N., Zukerberg, L., Nikolic, M., de la Monte, S., Dikkes, P., and Tsai, L. H. (1999). Conversion of p35 to p25 deregulates Cdk5 activity and promotes neurodegeneration. Nature *402*, 615–622.

Pei, J. J., Grundke-Iqbal, I., Iqbal, K., Bogdanovic, N., Winblad, B., and Cowburn, R. F. (1998). Accumulation of cyclin-dependent kinase 5 (cdk5) in neurons with early stages of Alzheimer's disease neurofibrillary degeneration. Brain Res. *797*, 267–277.

Pike, C. J., Walencewicz-Wasserman, A. J., Kosmoski, J., Cribbs, D. H., Glabe, C. G., and Cotman, C. W. (1995). Structure-activity analyses of beta-amyloid peptides: contributions of the beta 25–35 region to aggregation and neurotoxicity. J. Neurochem. *64*, 253–265.

Plattner, F., Angelo, M., and Giese, K. P. (2006). The roles of cyclin-dependent kinase 5 and glycogen synthase kinase 3 in tau hyperphosphorylation. J. Biol. Chem. *281*, 25457–25465.

Pocernich, C. B., Sultana, R., Mohmmad-Abdul, H., Nath, A., and Butterfield, D. A. (2005). HIV-dementia, Tat-induced oxidative stress, and antioxidant therapeutic considerations. Brain Res. Brain Res. Rev. *50*, 14–26.

Qu, D. *et al.* (2007). Role of Cdk5-mediated phosphorylation of Prx2 in MPTP toxicity and Parkinson's disease. Neuron *55*, 37–52.

Quintanilla, R. A., Orellana, D. I., Gonzalez-Billault, C., and Maccioni, R. B. (2004). Interleukin-6 induces Alzheimer-type phosphorylation of tau protein by deregulating the cdk5/p35 pathway. Exp. Cell Res. *295*, 245–257.

Robbins, E., and Gonatas, N. K. (1964). The ultrastructure of a mammalian cell during the mitotic cycle. J. Cell Biol. *21*, 429–463.

Rosales, J. L., and Lee, K. Y. (2006). Extraneuronal roles of cyclin-dependent kinase 5. Bioessays *28*, 1023–1034.

Sahlgren, C. M., Pallari, H. M., He, T., Chou, Y. H., Goldman, R. D., and Eriksson, J. E. (2006). A nestin scaffold links Cdk5/p35 signaling to oxidant-induced cell death. EMBO J. *25*, 4808–4819.

Sarkanen, J. R., Nykky, J., Siikanen, J., Selinummi, J., Ylikomi, T., and Jalonen, T. O. (2007). Cholesterol supports the retinoic acid-induced synaptic vesicle formation in differentiating human SH-SY5Y neuroblastoma cells. J. Neurochem. *102*, 1941–1952.

Shah, K., Liu, Y., Deirmengian, C., and Shokat, K. M. (1997). Engineering unnatural nucleotide specificity for Rous sarcoma virus tyrosine kinase to uniquely label its direct substrates. Proc. Natl. Acad. Sci. USA *94*, 3565–3570.

Shah, K., and Shokat, K. M. (2002). A chemical genetic screen for direct v-Src substrates reveals ordered assembly of a retrograde signaling pathway. Chem. Biol. *9*, 35–47.

Shah, K., and Shokat, K. M. (2003). A chemical genetic approach for the identification of direct substrates of protein kinases. Methods Mol. Biol. *233*, 253–271.

Shah, K., and Vincent, F. (2005). Divergent roles of c-Src in controlling platelet-derived growth factor-dependent signaling in fibroblasts. Mol. Biol. Cell *16*, 5418–5432.

Shaner, N. C., Steinbach, P. A., and Tsien, R. Y. (2005). A guide to choosing fluorescent proteins. Nat. Methods *2*, 905–909.

Sharma, M. R., Tuszynski, G. P., and Sharma, M. C. (2004). Angiostatin-induced inhibition of endothelial cell proliferation/apoptosis is associated with the down-regulation of cell cycle regulatory protein cdk5. J. Cell Biochem. *91*, 398–409.

Shaul, Y. D., and Seger, R. (2006). ERK1c regulates Golgi fragmentation during mitosis. J. Cell Biol. *172*, 885–897.

Shea, T. B., Zheng, Y. L., Ortiz, D., and Pant, H. C. (2004). Cyclin-dependent kinase 5 increases perikaryal neurofilament phosphorylation and inhibits neurofilament axonal transport in response to oxidative stress. J. Neurosci. Res. *76*, 795–800.

Shiraishi, T., Pankratova, S., and Nielsen, P. E. (2005). Calcium ions effectively enhance the effect of antisense peptide nucleic acids conjugated to cationic tat and oligoarginine peptides. Chem. Biol. *12*, 923–929.

Smith, P. D., O'Hare, M. J., and Park, D. S. (2004). Emerging pathogenic role for cyclin dependent kinases in neurodegeneration. Cell Cycle *3*, 289–291.

Song, J. H., Wang, C. X., Song, D. K., Wang, P., Shuaib, A., and Hao, C. (2005). Interferon gamma induces neurite outgrowth by up-regulation of p35 neuron-specific cyclin-dependent kinase 5 activator via activation of ERK1/2 pathway. J. Biol. Chem. *280*, 12896–12901.

Sridhar, J., Akula, N., and Pattabiraman, N. (2006). Selectivity and potency of cyclin-dependent kinase inhibitors. AAPS J. *8*, E204–E221.

Stanciu, M. *et al.* (2000). Persistent activation of ERK contributes to glutamate-induced oxidative toxicity in a neuronal cell line and primary cortical neuron cultures. J. Biol. Chem. *275*, 12200–12206.

Stepanichev, M. Y., Zdobnova, I. M., Yakovlev, A. A., Onufriev, M. V., Lazareva, N. A., Zarubenko, I. I., and Gulyaeva, N. V. (2003). Effects of tumor necrosis factor-alpha central administration on hippocampal damage in rat induced by amyloid beta-peptide (25–35). J. Neurosci. Res *71*, 110–120.

Strocchi, P., Pession, A., and Dozza, B. (2003). Up-regulation of cDK5/p35 by oxidative stress in human neuroblastoma IMR-32 cells. J. Cell Biochem. *88*, 758–765.

Strock, C. J., Park, J. I., Nakakura, E. K., Bova, G. S., Isaacs, J. T., Ball, D. W., and Nelkin, B. D. (2006). Cyclin-dependent kinase 5 activity controls cell motility and metastatic potential of prostate cancer cells. Cancer Res. *66*, 7509–7515.

Sutterlin, C., Hsu, P., Mallabiabarrena, A., and Malhotra, V. (2002). Fragmentation and dispersal of the pericentriolar Golgi complex is required for entry into mitosis in mammalian cells. Cell *109*, 359–369.

Sutterlin, C., Lin, C. Y., Feng, Y., Ferris, D. K., Erikson, R. L., and Malhotra, V. (2001). Polo-like kinase is required for the fragmentation of pericentriolar Golgi stacks during mitosis. Proc. Natl. Acad. Sci. USA *98*, 9128–9132.

Takahashi, M., Iseki, E., and Kosaka, K. (2000). Cdk5 and munc-18/p67 co-localization in early stage neurofibrillary tangles-bearing neurons in Alzheimer type dementia brains. J. Neurol. Sci. *172*, 63–69.

Takashima, A., Murayama, M., Yasutake, K., Takahashi, H., Yokoyama, M., and Ishiguro, K. (2001). Involvement of cyclin dependent kinase5 activator p25 on tau phosphorylation in mouse brain. Neurosci. Lett. *306*, 37–40.

Tsai, L. H., Delalle, I., Caviness, V. S., Jr., Chae, T., and Harlow, E. (1994). p35 is a neural-specific regulatory subunit of cyclin-dependent kinase 5. Nature *371*, 419–423.

Tsai, L. H., Lee, M. S., and Cruz, J. (2004). Cdk5, a therapeutic target for Alzheimer's disease? Biochim. Biophys. Acta *1697*, 137–142.

Walker, A., Ward, C., Sheldrake, T. A., Dransfield, I., Rossi, A. G., Pryde, J. G., and Haslett, C. (2004). Golgi fragmentation during Fas-mediated apoptosis is associated with the rapid loss of GM130. Biochem. Biophys. Res. Commun. *316*, 6–11.

Wei, W., Wang, X., and Kusiak, J. W. (2002). Signaling events in amyloid beta-peptide-induced neuronal death and insulin-like growth factor I protection. J. Biol. Chem. *277*, 17649–17656.

Xie, S., Wang, Q., Ruan, Q., Liu, T., Jhanwar-Uniyal, M., Guan, K., and Dai, W. (2004). MEK1-induced Golgi dynamics during cell cycle progression is partly mediated by Polo-like kinase-3. Oncogene *23*, 3822–3829.

Xiong, W., Pestell, R., and Rosner, M. R. (1997). Role of cyclins in neuronal differentiation of immortalized hippocampal cells. Mol. Cell Biol. *17*, 6585–6597.

Yamaguchi, H., Ishiguro, K., Uchida, T., Takashima, A., Lemere, C. A., and Imahori, K. (1996). Preferential labeling of Alzheimer neurofibrillary tangles with antisera for tau protein kinase (TPK) 1/glycogen synthase kinase-3 beta and cyclin-dependent kinase 5, a component of TPK II. Acta Neuropathol. *92*, 232–241.

Yan, G. Z., and Ziff, E. B. (1995). NGF regulates the PC12 cell cycle machinery through specific inhibition of the Cdk kinases and induction of cyclin D1. J. Neurosci. *15*, 6200–6212.

Yankner, B. A., Duffy, L. K., and Kirschner, D. A. (1990). Neurotrophic and neurotoxic effects of amyloid beta protein: reversal by tachykinin neuropeptides. Science *250*, 279–282.

Zheng, Y. L., Kesavapany, S., Gravell, M., Hamilton, R. S., Schubert, M., Amin, N., Albers, W., Grant, P., and Pant, H. C. (2005). A Cdk5 inhibitory peptide reduces tau hyperphosphorylation and apoptosis in neurons. EMBO J. *24*, 209–220.

Zheng, Y. L., Li, B. S., Amin, N. D., Albers, W., and Pant, H. C. (2002). A peptide derived from cyclin-dependent kinase activator (p35) specifically inhibits Cdk5 activity and phosphorylation of tau protein in transfected cells. Eur. J. Biochem. *269*, 4427–4434.

Zheng, Y. L., Li, B. S., Kanungo, J., Kesavapany, S., Amin, N., Grant, P., and Pant, H. C. (2007). Cdk5 Modulation of mitogen-activated protein kinase signaling regulates neuronal survival. Mol. Biol. Cell *18*, 404–413.